Molecular and Cellular Endocrinology 590 (2024) 112272

Contents lists available at ScienceDirect

Molecular and Cellular Endocrinology

journal homepage: www.elsevier.com/locate/mce

Cellular landscape of adrenocortical carcinoma at single-nuclei resolution

David S. Tourigny [a,*,1], Barbara Altieri [b,1], Kerim A. Secener [c,d], Silviu Sbiera [b], Marc P. Schauer [b,e], Panagiota Arampatzi [f], Sabine Herterich [g], Sascha Sauer [c], Martin Fassnacht [b], Cristina L. Ronchi [h,i,**]

[a] School of Mathematics, University of Birmingham, Birmingham, B15 2TT, UK
[b] Division of Endocrinology and Diabetes, University Hospital of Würzburg, Würzburg, 97080, Germany
[c] Max Delbrück Center for Molecular Medicine, Berlin, 13125, Germany
[d] Institute of Biochemistry, Department of Biology, Chemistry and Pharmacy, Free University Berlin, Berlin, 14195, Germany
[e] Center for Cellular Immunotherapy, Department of Internal Medicine II, University Hospital of Würzburg, Würzburg, 97080, Germany
[f] Core Unit SysMed, University of Würzburg, Würzburg, 97080, Germany
[g] Central Laboratory, University Hospital of Würzburg, Würzburg, 97080, Germany
[h] Institute of Metabolism and System Research, University of Birmingham, Birmingham, B15 2TT, UK
[i] Centre for Endocrinology, Diabetes and Metabolism (CEDAM), Birmingham Health Partners, Birmingham, B15 2GW, UK

ARTICLE INFO

Keywords:
Adrenal gland
Cancer
Molecular oncology
Single cell
Tissue homeostasis

ABSTRACT

Adrenocortical carcinoma (ACC) is a rare yet devastating tumour of the adrenal gland with a molecular pathology that remains incompletely understood. To gain novel insights into the cellular landscape of ACC, we generated single-nuclei RNA sequencing (snRNA-seq) data sets from twelve ACC tumour samples and analysed these alongside snRNA-seq data sets from normal adrenal glands (NAGs). We find the ACC tumour microenvironment to be relatively devoid of immune cells compared to NAG tissues, consistent with known high tumour purity values for ACC as an immunologically "cold" tumour. Our analysis identifies three separate groups of ACC samples that are characterised by different relative compositions of adrenocortical cell types. These include cell populations that are specifically enriched in the most clinically aggressive and hormonally active tumours, displaying hallmarks of reorganised cell mechanobiology and dysregulated steroidogenesis, respectively. We also identified and validated a population of mitotically active adrenocortical cells that strongly overexpress genes *POLQ*, *DIAPH3* and *EZH2* to support tumour expansion alongside an *LGR4*+ progenitor-like or cell-of-origin candidate for adrenocortical carcinogenesis. Trajectory inference suggests the fate adopted by malignant adrenocortical cells upon differentiation is associated with the copy number or allelic balance state of the imprinted *DLK1/MEG3* genomic locus, which we verified by assessing bulk tumour DNA methylation status. In conclusion, our results therefore provide new insights into the clinical and cellular heterogeneity of ACC, revealing how genetic perturbations to healthy adrenocortical renewal and zonation provide a molecular basis for disease pathogenesis.

1. Introduction

Adrenocortical carcinoma (ACC) is a rare yet highly aggressive tumour of the adrenal gland (annual incidence 0.7–2 cases per million in USA; 5-year survival 50–60% early stage detection, 10–30% in later stages) with a molecular pathology that remains incompletely understood, which poses significant management challenges (Libé, 2019; Juhlin et al., 2021; Lerario et al., 2022; Altieri et al., 2020; Lippert et al., 2023). ACC is often associated with hypersecretion of various adrenocortical steroid hormones (usually cortisol and androgens) although can also be endocrinologically inactive meaning that clinical detection can be delayed until the later stages of disease (Fassnacht et al., 2018). ACC presents most frequently as sporadic, but can be associated with genetic syndromes in approximately 3–5% of cases (Fassnacht et al., 2018; Lloyd

* Corresponding author. School of Mathematics, University of Birmingham, Birmingham, B15 2TT, UK.
** Corresponding author. Institute of Metabolism and System Research, College of Medical and Dental Science, University of Birmingham, Birmingham, B15 2TT, UK.
E-mail addresses: d.tourigny@bham.ac.uk (D.S. Tourigny), c.l.ronchi@bham.ac.uk (C.L. Ronchi).
[1] These authors contributed equally to this work and are co-first authors.

https://doi.org/10.1016/j.mce.2024.112272
Received 11 March 2024; Received in revised form 8 May 2024; Accepted 14 May 2024
Available online 15 May 2024

et al., 2017). Histological diagnosis of sporadic ACC is based on the modified Weiss scoring criteria, which includes parameters on tumour architecture, mitosis, and tumour invasion (Weiss et al., 1989; Mete et al., 2022). Immunohistochemistry (IHC) has proved an invaluable diagnostic and prognostic companion tool, and current practice is based on the use of markers including steroidogenic factor 1 (SF1) to recognise the adrenal origin of the tissue and the Ki-67 proliferation index to define the aggressiveness of the tumour (Mete et al., 2018, 2022; Papathomas et al., 2016; Sbiera et al., 2010; Beuschlein et al., 2015).

Recent integrative (Assié et al., 2014) and pan-genomic (Zheng et al., 2016) analyses have investigated the molecular attributes of sporadic ACC, with the latter contributing to The Cancer Genome Atlas ACC project (TCGA-ACC). These studies have highlighted a role for whole genome duplication and large-scale chromosomal copy number variations (CNVs), as well as near-ubiquitous overexpression of *IGF2* through loss of heterozygosity (LOH) or aberrant methylation of the maternal allele at the imprinted locus 11p15.5. Using Cluster of Cluster (COC) analysis of integrated genomic, DNA methylation, messenger RNA (mRNA) and micro-RNA (miRNA) expression data, three molecular subtypes of sporadic ACC were proposed to be consistent with grading based on histology and IHC (Zheng et al., 2016). Specifically, molecular subtype COC3 contained the most aggressive tumours, with COC1 showing the most favourable clinical outcome and COC2 presenting an intermediate prognosis.

Sporadic ACC is characterised by cancer initiating events that occur during homeostatic maintenance or renewal of post-developmental adrenocortical tissue (Yates et al., 2013; Kim and Choi, 2020). The human adrenal cortex is composed of three concentric zones of cells responsible for synthesising three different sets of steroid hormones: the outer zona glomerulosa (ZG, mineralocorticoids), zona fasciculata (ZF, glucocorticoids) and the inner zona reticularis (ZR, androgens). Maintenance and renewal of this zonation is believed to involve at least one adult stem cell population sustained by a gradient of WNT signalling concentrated near the outer capsule, which becomes replaced by an increasing gradient of Protein Kinase A (PKA) signalling as cells are displaced to undergo centripetal migration and differentiation (Chang et al., 2013; Pignatti et al., 2017; Little et al., 2021). Exact mechanisms by which WNT and PKA signals interact to generate the different adrenocortical zonal cell types remain incompletely understood, but WNT modulators together with phosphodiesterase enzymes (PDEs) are suggested to achieve this balance by controlling intracellular levels of β-catenin and cAMP, respectively (Vidal et al., 2016; Drelon et al., 2016a; Mathieu et al., 2018; Basham et al., 2019; Pignatti et al., 2020). Such a model is consistent with findings that mutations in WNT and PKA pathways are among the most commonly-occurring somatic events associated with various lesions of the adrenal cortex (Juhlin et al., 2021; Assié et al., 2014; Zheng et al., 2016; Penny et al., 2017).

Although great progress has been made towards delineating the molecular mechanisms of adrenocortical development, maintenance, renewal and pathogenesis in humans, very little remains known about the landscape of cell types involved in these processes. Notable exceptions include recent single-cell and single-nuclei studies on the foetal (del Valle et al., 2023) and our own study on the adult (Altieri et al., 2022) human adrenal gland, respectively. While the latter also includes data from a cohort of adrenocortical adenoma (ACA) samples, equivalent data on ACC have hitherto been lacking. To better understand the composition of cell types and mechanisms involved in ACC pathogenesis, in the present study we assembled and analysed a cellular transcriptome atlas using single-nuclei transcriptomic sequencing (snRNA-seq) on tissue samples from a cohort of ACC patients.

2. Materials and Methods

2.1. Patients and clinical details

Demographic, clinical and histopathological data for the eight patients with ACC included in the present study were collected from patients' records and are summarised in Table 1. Diagnosis of ACC was histologically confirmed according to the current European guidelines (Fassnacht et al., 2018). Baseline ENSAT tumour stage, as well as Weiss score and Ki-67 proliferation index of the analysed tissues were collected. Steroid hormone levels were measured at the time of surgery (i.e., at resection of tumour tissue evaluated in the present study) using commercially available analytical procedures as previously reported (Detomas et al., 2021). Table 1 also includes the demographic characteristics of six subject with NAG deriving from the tissue surrounding endocrine inactive adenomas (EIA) or from adrenalectomies performed during surgery for renal cell carcinoma, which were included in a previous snRNA-seq study (Altieri et al., 2022) and used as reference. Samples from patients PACCm-1 and PACCm-2 were isolated from metastatic lesions of the peritoneum and perirenal lymph node, respectively. The study was approved by the ethics committee of the University of Würzburg (No. 93/02 and 88/11) and written informed consent was obtained from all subjects.

2.2. Sample selection, preparation, and snRNA sequencing

Nuclei were isolated from snap-frozen samples derived from ACC tissue dissected by an expert pathologist and obtained during tumour resection using the protocol previously described in (Altieri et al., 2022; Krishnaswami et al., 2016). Quality and purity of isolated nuclei were confirmed by microscopy and yield was quantified using a Neubauer chamber. Salinisation, reverse transcription (RT) and library preparation were performed according to the inDrop™ system from 1CellBio (Baron et al., 2016) on chips with hydrogel beads, with library preparation following the CEL-Seq2 protocol (Hashimshony et al., 2016) where the RT product was first digested by ExoI and HinFI and purified using AMpure XP beads (Beckman Coulter, USA). cDNA was quantified by qPCR (Roche Light Cycler 480 Instrument II, Switzerland) and pooled for sequencing using an Illumina HiSeq 2000 instrument with 60 bases for read 1, 6 for the Illumina index, and 50 for read 2.

2.3. snRNA-seq data processing and analysis

FASTQ files containing raw snRNA-seq reads were generated using the Illumina bcl2fastq tool and processed with the zUMI pipeline (version 2.5 – default parameters) (Parekh et al., 2018). Count matrices were then used as input into Seurat (version 4.2) (Butler et al., 2018), which was used to create objects for all downstream processing and analysis in the *R* programming language. Initial quality control included filtering out cells that contained less than 100 or more than 2500 features, or more than 4000 total counts, after removing genes that mapped to ribosomal and mitochondrial coding or pseudo coding regions. We also repeated the analyses without removing these genes to confirm that this step did not affect the scientific conclusions of this paper.

Normalisation was performed on a sample-by-sample basis using the Seurat function SCTransform(), and initial cell types for ACC samples were predicted the merged data set of NAG samples as a reference with the Seurat functions FindTransferAnchors() and TransferData(), as described by the Seurat vignettes available online at the time. Following initial cell type predictions, normalised count matrices for ACC and NAG samples were merged and unsupervised clustering (resolution = 0.1) was performed using the top 30 principal components. Differential gene expression (DGE) analysis performed on merged data using the Seurat function FindAllMarkers() provided a second route to initial cell type identification, and cells without a consistent annotation in both methods were excluded from downstream analysis. The filtered count matrices obtained after excluding these cells were then renormalised and remerged to create a final count matrix that was used for unsupervised clustering (resolution = 0.6) and final annotation of cell types based on DGE and hallmark gene set analysis. Pearson correlation coefficients were calculated for all sample pairs by using the Seurat function

Table 1
Demographic, clinical, and hormonal characteristics for the eight patients with adrenocortical carcinoma (ACC) and the six subjects with removed normal adrenal glands (NAG) included in the study. Abbreviations: ACC, adrenocortical carcinoma; M, male; F, female; NA, not applicable; NAGE, normal adrenal gland deriving from endocrine inactive adenoma (EIA); NAGR, normal adrenal gland deriving from renal cell carcinoma (RCC); NGS, next generation sequencing. *Cases sequenced twice.

Patient ID	Diagnosis	Sex	Age at surgery	ENSAT tumour stage at the time of diagnosis	Type of surgery	Hormone pattern at time of tissue sampling	DNA sequencing	Somatic variants in the analysed tissue (gene names)	Tumour size of the analysed tissue (mm)	Ki-67% of the analysed tissue
PACCp-1	ACC	F	36	3	Primary	Cortisol & androgens	Targeted NGS	*TP53*	170	20
PACCp-2*	ACC	F	72	1	Primary	Cortisol & androgens	Targeted NGS	*CTNNB1*	50	15
PACCp-3	ACC	F	66	2	Primary	Cortisol & androgens	Targeted NGS	*APC, NF1*	82	10
PACCp-4*	ACC	M	71	1	Primary	Estrogen	Targeted NGS	*KDM6A1, RB1, TP53*	45	40
PACCr-1*	ACC	F	38	unknown	Recurrence	Cortisol	Sanger seq	WT for *CTNNB1, GNAS* and *PKA*	35	unknown
PACCr-2	ACC	F	61	2	Recurrence	Endocrine inactive	Targeted NGS	none	94	15
PACCm-1*	ACC	F	56	3	Metastasis	Cortisol & androgens	Sanger seq	WT for *CTNNB1, GNAS* and *PKA*	100	unknown
PACCm-2	ACC	F	45	1	Metastasis	Endocrine inactive	Targeted NGS	*KDR, MEN1, ZNRF3*	25	50
PNAGe-1	NAG from EIA	F	54	NA	NA	NA	NA	NA	NA	NA
PNAGe-2*	NAG from EIA	F	49	NA	NA	NA	NA	NA	NA	NA
PNAGe-3	NAG from EIA	M	71	NA	NA	NA	NA	NA	NA	NA
PNAGr-1	NAG from RCC	M	56	NA	NA	NA	NA	NA	NA	NA
PNAGr-2*	NAG from RCC	M	81	NA	NA	NA	NA	NA	NA	NA
PNAGr-3	NAG from RCC	M	68	NA	NA	NA	NA	NA	NA	NA

AverageExpression() to generate an averaged gene expression profile for each sample.

Gene set scores for cell types were calculated based on a customised version of single-cell gene set analysis by adapting the Seurat functions AddModuleScore() and FindAllMarkers() as previously described in (Tourigny et al., 2022). Log ratio-of-proportions (log ROP) scores were obtained by dividing by the total number of cells in either sample type (ACC or NAG) and then taking the natural logarithm of the ratio of these proportions within each cell type. To calculate the Shannon entropy of each cell type, proportions were instead calculated on a patient basis after removing NAG samples and the function Entropy() from the *R* package DescTools was applied. Slingshot (Street et al., 2018) was used according to the authors instructions by applying the functions getLineages() and SlingshotDataSet() with default settings for trajectory inference. The version of the StemID score used in this study is equivalent to that described in (Grün et al., 2016) where the estimated transcriptome entropy (with lowest entropy subtracted) for each cell type is multiplied by the number of links extending from that cell type as reported by Slingshot.

2.4. Immunohistochemistry

Formalin-fixed paraffin-embedded (FFPE) slides of 79 adrenal tissues, including 68 ACC and 11 NAG were used to validate the expression of *DIAPH3* and *POLQ* at protein levels by immunohistochemistry (IHC). IHC was performed as previously reported (Altieri et al., 2022).

2.5. Methylation status multiplex-ligation dependent probe amplification

Methylation status multiplex-ligation dependent probe amplification (MS-MLPA) was performed according to the manufacturer's protocol using SALSA MS-MLPA Probemix ME032-B1 UPD7-UPD14-v03. The probe mix contains 14 reference probes and 32 specific probes for the regions 7p12.2, 7q32.2, 14q32.2 and 14q32.31, including the *GRB10*, *MEST*, *DLK1*, *MEG3* and *RTL1* genes. Ten of these specific probes contain a *Hha*I recognition site and provide information about the methylation status. 150 ng of DNA were used in each MS-MLPA reaction.

Hybridisation, ligation and PCR were performed in a Biometra 96-well PCR thermal cycler. Fragment separation was done by capillary electrophoresis on a CEQ8000 capillary sequencer (ABSciex). Peaks were size-called and assigned to MLPA-probes by GenomLab GeXP-Fragment Analysis software. Quality checking covered DNA concentration, MLPA-reaction, DNA-denaturation and *Hha*I-digestion. Peak height in relative fluorescence units (rfu) was used for quantification. After normalisation, dosage quotients were calculated and compared between amplification products of the digested versus the undigested sample.

2.6. Statistical analysis

All customised statistical tests reported in the main text were performed in the *R* programming language. Adjusted p values for marker genes and gene set scores were obtained using the Seurat function FindAllMarkers (), which uses a Wilcoxon signed-rank test with Bonferroni adjustment. The prop.test() function (default values) was used to test the null hypothesis that proportions of cell populations in two groups of samples are the same, with a two-sided alternative distribution and confidence level of 95%. Gene set variation analysis (GSVA) (Hänzelmann et al., 2013) was used to score TCGA-ACC samples by cell type signatures derived from marker gene sets. The comparison of means of multiple sample groups was performed using an ANOVA test implemented in the function stat_compare_means() and p values for comparisons of pairs of groups were calculated using Wilcox method. Absolute p values for paired comparisons are reported in the main text while the annotations "*", "**", "***" and "****" have been used to denote p values less than 0.05, 0.01, 0.001 and 0.0001 in figures, respectively. Prognostic values of genes of interest were evaluated using a 0.25/0.75 proportion hazard ratio (HR) with bulk TCGA-ACC RNA-seq and overall survival data as described in (Xie et al., 2019).

3. Results

3.1. Cellular landscape of adrenocortical carcinomas

We conducted snRNA-seq on twelve tumour samples (six primary, three metastatic and three recurrent tissues) from a total of eight patients (7F/1M, median age 58.5 yrs) with histologically confirmed diagnosis of ACC (Table 1 and Materials and Methods). Patients displayed a variety of steroid profiles at the time of resection, including four with mixed cortisol and androgens excess, one with cortisol excess alone, two with endocrine inactive tumours, and a single male patient with a rare, estrogen-secreting tumour. The genomic backgrounds of tumour samples in the study included alterations in genes frequently mutated in ACC, including *TP53*, *CTNNB1* and *ZNRF3* (Table 1 and (Zheng et al., 2016)).

Following quality control and removal of genes mapping to mitochondrial and ribosomal genes, normalisation and variance stabilisation of the count matrices were performed using Seurat (Butler et al., 2018). Initial cell types were predicted for each sample individually using a merged snRNA-seq data set from six normal adrenal glands (NAGs) from a previous study from our group as a reference (Altieri et al., 2022). These cell types are found to contain cells of adrenocortical origin together with adrenal medullary cells (**AM**), myeloid cells (**MC**), lymphoid cells (**LC**), fibroblast and connective tissue cells (**FC**), and vascular and endothelial cells (**VEC**). We then compared initial cell type predictions with annotations based on the same six cell types but informed by DGE analysis, performed following principal component analysis and unsupervised clustering after merging normalised count matrices for all ACC and NAG samples (Materials and Methods). Both sample-based and merged approaches to cell type inference confirm multiple cell populations with adrenocortical origin and a relative depletion of immune cell types in ACC compared to NAG (Fig. S1), in line with reports of high tumour purity, high heterogeneity and low immune and stromal infiltration in ACC (Zheng et al., 2016; Thorsson et al., 2018; Landwehr et al., 2020). However, we highlight that immune depletion could be minimally exacerbated by snRNA-seq experimental preparation procedures by selectively excluding certain cell types.

Excluding cells with inconsistent annotations resulted in a final total of 39,364 cells for downstream analysis. We renormalised and remerged ACC and NAG count matrices for these cells, performing unsupervised clustering at higher resolution to reveal a total of 19 cellular clusters (Fig. 1A). To identify the nature of cell types, DGE analysis was combined with a calculation of the log ROP score of ACC to NAG cells within each cluster (Fig. 1B) (Materials and Methods). Using the rationale that a higher log ROP score is indicative of a higher proportion of cells derived from cancer samples, we identified eight adrenocortical cell types (**ACC 1–5**, **ACC E1, E2** and **ACC M**) that appear to be specific to ACC. Conversely, clusters with a low log ROP score included infiltrating cell types, medullary cells and two adrenocortical cell types identified with **ZG** and **ZR**, based on expression of known markers such as *DACH1* and *SULT2A1*, respectively (Table S1) (Altieri et al., 2022). Four remaining adrenocortical cell types, which contained approximately equal proportions of cells from ACC and NAG samples (Fig. 1B), are identified as representing a progressive continuum of cell types from the ZF - based on expression of cytochrome P450 *CYP17A1* (**ZF 1**) and non-canonical NOTCH ligand *DLK1* (**ZF 2** and **ZF 3**) (Altieri et al., 2022; Hadjidemetriou et al., 2019) - and a comparatively undifferentiated adrenocortical zone (**UZ**) expressing very few known marker genes (Table S1).

Correlation coefficients based on average gene expression profiles revealed the strongest degree of similarity between pairs of ACC samples originating from the same patient, suggesting higher levels of inter- than intra-tumour heterogeneity, whereas inter-patient heterogeneity was

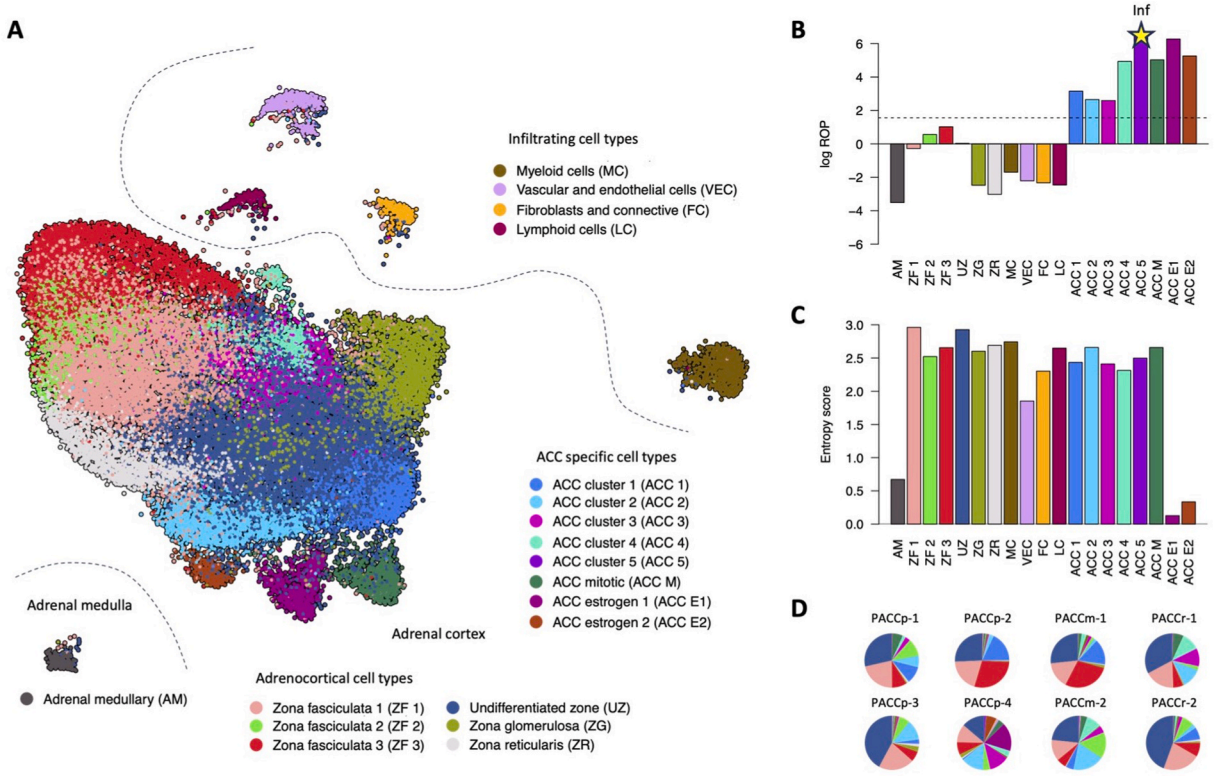

Fig. 1. Landscape of cell types in ACC. (A) UMAP projection showing all cells in the merged data set of ACC and NAG samples, coloured by cell type. (B) Bar plot of log ROP scores (see Materials and Methods for details) for each cell type where the dotted line serves as a rough guide above which those that fall were denoted ACC specific. Note that **ACC 5** consists entirely of cells from ACC samples meaning that its log ROP score is infinitely large. (C) Bar plot of patient-based Shannon entropy score (see Materials and Methods for details), indicating the degree to which each cell type is patient specific. (D) Pie charts showing a different representation of the distribution of cell types among the eight ACC patients included in this study (see Table 1 for details).

comparably lower across NAG tissues (Fig. S2). To quantify the distribution of cell types across ACC patients, we calculated a score based on Shannon entropy (Fig. 1C) (Materials and Methods). Cell types that are highly specific to one patient have an entropy score close to zero, while the entropy score increases as cell clusters become distributed across patients. Two cell types with the lowest entropy score (**ACC E1** and **ACC E2**) are found to consist almost exclusively of cells (99.3% and 97.7%, respectively) from case PACCp-4 who was the only male patient in our cohort and had clinically excessive circulating estrogen levels at the time of resection (Fig. 1D). By comparison, the remaining six ACC specific cell types have higher entropy scores, reflecting the fact that they are represented in tumours from multiple patients in the study (Fig. 1D).

3.2. Characterisation of ACC specific cell types

Different ACC specific cell types were characterised using MSigDB hallmark gene set scores and identification of marker genes based on DGE analysis (Fig. 2 and Tables S1 and S2) (Materials and Methods). **ACC 1** cells score highest for *ANGIOGENESIS* but are most significantly enriched for the gene set *EPITHELIAL MESECHYMAL TRANSITION* (EMT) (adjusted p = 1.16e-82) and correspondingly their top marker genes (as ranked by p value) includes factors involved in cellular mechanics or motility (*SPOCK1, COL11A1, CTNNA2, NTM*, *SLIT2*, *DCN*) and calcium signalling (*CALN1*, *CADPS, CACNA2D1, CACNB2*) (Fig. 2B and Table S1), consistent with the role of calcium in regulating cytoskeletal and cell-matrix interactions during the EMT (Tsai et al., 2015; Janke et al., 2023). However, many genes from the EMT gene set are not among the top markers for **ACC 1** cells, which likely explains why the prognostic value of this pathway in ACC is limited (Sbiera et al., 2021). **ACC 2**, **ACC 3**, and **ACC 4** cells were differentiated by their metabolic characteristics: **ACC 2** cells score most significantly for the gene set *CHOLESTEROL HOMEOSTASIS* (adjusted p = 3.75e-203), consistent with top marker genes including those involved in cholesterol transport (*GRAMD1B*, *LDLR, SCARB1*), the mevalonate pathway (*HMGCS1*, *HMGCR*), sterol biosynthesis (*SQLE*, *FDPS*, *FDFT1, MSMO1*) and early steps in steroid hormone synthesis (*CYP11A1*, *FDX1*) (Fig. 2B and Table S1). The top marker genes for **ACC 3** are acyl-CoA synthetase *ACSM3* and *THUMPD1* (average log2 fold change = 1.36 and 0.71, respectively, adjusted p < 2.3e-308) (Fig. 2B and Table S1), whereas **ACC 4** scores highest for the gene sets *HYPOXIA* and *GLYCOLYSIS* (adjusted p = 6.11e-175 and 7.31e-108, respectively) (Fig. 2A and Table S2). As displayed in Fig. 2B, cells from **ACC 4** correspondingly express the vascular endothelial growth factor *VEGFA* and glycolytic genes such as *PGK1* among other top marker genes (average log2 fold change = 0.47 and 0.45, adjusted p = 5.15e-171 and 5.68e-165, respectively) while the VEGFR receptor gene *FLT1* is a top marker gene for the endothelial cell cluster **VEC** (average log2 fold change = 0.73, adjusted p < 2.3e-308). This suggests that **ACC 4** represents a cell type that actively stimulates glycolysis and angiogenesis in response to hypoxic signals, recently explored in (Oliveira et al., 2022). **ACC E1** and **ACC E2** cells specific to patient PACCp-4 score most significantly for the gene sets *ESTROGEN RESPONSE EARLY* and *EMT* (adjusted p = 3.49e-30 and 4.31e-27, respectively) and *G2M CHECKPOINT* and *CHOLESTEROL HOMEOSTASIS* (adjusted p = 6.32e-9 and 2.00e-08, respectively), respectively, and similarly share a subset of marker genes with the major ACC specific clusters **ACC 1–4** (Fig. 2B and Table S1).

The two remaining ACC specific cell types, **ACC 5** and **ACC M**, display hallmarks of proliferative and mitotic activity, respectively. **ACC 5** is the cell type with by far the smallest representation in our data set (just 77 out of 39,364, less than 0.2 % cells) and its top markers include genes for marker of proliferation Ki-67 (*MKI67*) (average log2 fold change = 0.20, adjusted p = 4.5e-67) and components of the WNT (*LGR4*) and NOTCH signalling (*JAG1*) pathways (average log2 fold change = 0.29 and 0.25, adjusted p = 3.09e-08 and 0.0015, respectively), along with transcriptional factors such as *NFE2L3*, *SOX4* and the glucocorticoid receptor (*NR3C1*) (average log2 fold change = 0.36, 0.21 and 0.26, adjusted p = 3.86e-114, and 0.00016,respectively) that are important for determining cell fate in response to para- or endocrine signals (Fig. 2B and Table S1) (Wilson and Koopman, 2002; Hollenberg et al., 1985; Saliba et al., 2022; Glinka et al., 2011; Li et al., 1997). Correspondingly, **ACC 5** cells score significantly for the gene sets *G2M CHECKPOINTS, TGF BETA SIGNALING*, *WNT BETA CATENIN-SIGNALING* and *NOTCH SIGNALING* (adjusted p = 4.29e-11, 2.02e-06, 0.007 and 0.009, respectively) (Fig. 2A and Table S2). By comparison, **ACC M** contains almost ten-fold more representatives in our data set (734 out of 39,364, 1.9 % cells) and the top protein coding marker genes for this cell type are *DIAPH3* (diaphanous related formin 3) and *POLQ* (average log2 fold change = 0.46 and 0.35, respectively, adjusted p < 2.3e-308) as shown in Fig. 2B and Table S1. *POLQ* is a DNA polymerase (Sharief et al., 1999), and *DIAPH3* was recently reported to localise to the centrosome and regulate the assembly and bipolarity of the mitotic spindle during mitosis (Lau et al., 2021), which is consistent with indications that **ACC M** cells are actively engaged in mitotic activity. Correspondingly, they score most significantly enriched for the three gene sets *E2F TARGETS*

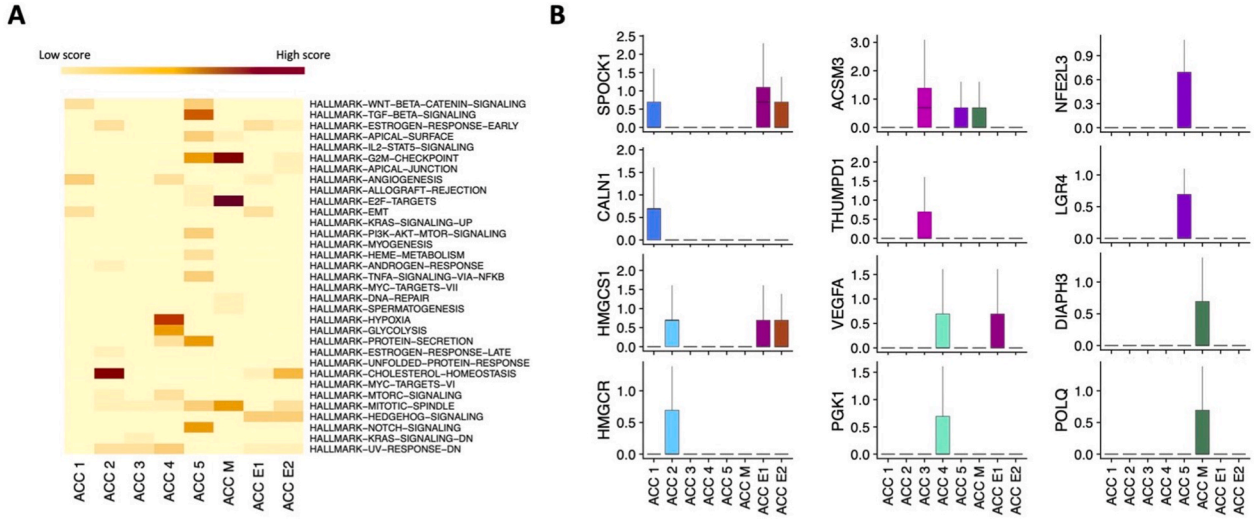

Fig. 2. Characterisation of ACC specific cell types. (A) Heatmap of hallmark gene set scores for each ACC specific cell type (see Materials and Methods for details), coloured with a gradient from zero (lowest) to one (dark red). (B) Plots of selected top marker genes for each ACC specific cell type, where the vertical axis shows (SCT normalised) level of expression for the corresponding gene.

(adjusted p < 2.3e-308), *G2M CHECKPOINTS* (adjusted p = 3.07e-213) and *MITOTIC SPINDLE* (adjusted p = 3.23e-80) (Fig. 2A and Table S2).

Since **ACC M** cells are found in relatively high numbers across all ACC samples while being almost entirely absent from NAG (high log ROP and entropy scores, Fig. 1B and C), we investigated the possibility of using their top marker genes to distinguish ACC from normal or benign adrenocortical tissue at the bulk level. Both *POLQ* and *DIAPH3* were found to be significantly overexpressed in bulk RNA from ACC samples compared to NAG and ACA tissue, as reproduced in two different available data sets (Fig. 3A and Fig. S3) (Di et al., 2020; Giordano et al., 2009). We next validated the expression of both *POLQ* and *DIAPH3* at the protein level using IHC in a large cohort of ACC (n = 68) and NAG tissue samples (n = 11) (see Material and Methods and Table S3 for details). Hereby we found that these proteins mark populations of cells that are found at significantly higher levels in ACC compared to NAG (mean POLQ H-score ± Standard deviation (SD) = 135.6 ± 62.6 for ACC versus 73.5 ± 32.4 for NAG, respectively, p = 0.0017; mean DIAPH3 H-score ± SD = 204.4 ± 50.9 for ACC versus 95.1 ± 25.6 for NAG, respectively, p = 1.6e-06) (Fig. 3B). We also confirmed using TCGA-ACC data that both *DIAPH3* and *POLQ* high expression is strongly associated with lower overall survival (HR 8.01 and 7.68 with 95% confidence interval (CI) [3.3,19.3] and [3.3,17.6], respectively; p < 2.2e-16). Taken together, these results suggest that **ACC M** represents a population of mitotic adrenocortical cells that are generously and reproducibly enriched within malignant adrenocortical tumours. Of note, **ACC M** cells also strongly express the histone methyltransferase *EZH2* that has also been shown to play a key role in adrenocortical cell differentiation and aggressiveness in ACC (Mathieu et al., 2018; Tabbal et al., 2019; Drelon et al., 2016b).

3.3. Cellular compositions of molecular ACC subtypes

We next performed hierarchical clustering based on cell type composition, which separates out NAG samples and partitioned ACC samples into three distinct groups (I, II and III) that mixed primary, recurrence and metastatic lesions (Fig. 4A). Mixing of different lesion types within the same group implies that individual cellular profiles are faithfully reproduced across different stages of carcinogenesis, which complements recent comparative studies on the genomic landscapes of metastatic and primary tumours (Gara et al., 2018; Fojo et al., 2020). Samples from group II are characterised by a significantly higher proportion of **ACC 1** cells than groups I and III (p < 2.2e-16; 95% CI [14.8%, 16.3%] and [8.9%,10.9%] greater than groups I and III, respectively). Conversely, group I, which included samples from patient PACCp-4, is enriched for **ACC 2** cells (p < 2.2e-16; 95% CI [10.6%,12.1%] and [5.5%,7.5%] greater than groups II and III, respectively) while group III has no significant difference in the proportions of **ACC 1** and **ACC 2** (p = 0.45). Group I samples also have significantly higher proportions of the four remaining ACC specific cell types: **ACC 3**, **ACC 4**, **ACC 5** and **ACC M** (p < 2.2e-16; 95% CI [17.3%,19.2%] and [15.8%,17.9%] greater than groups II and III, respectively).

To assess whether molecular ACC subtypes reflect associations with different cellular subpopulations, we generated single-cell signatures by taking the top 20 protein coding marker genes for each ACC specific cell type and used them to score TCGA-ACC samples based on GSVA (Hänzelmann et al., 2013) (Materials and Methods). COC3 samples scored significantly higher than COC1 samples for both **ACC 1** and **ACC 2** signatures (p = 0.00053 and 0.021, respectively) as did COC2 for **ACC 1** (p = 0.019) (Fig. 4B), suggesting these gene signatures are enriched in the more aggressive COC3 and intermediate COC2 ACC subtypes. By contrast, COC1 samples scored significantly higher than COC 3 samples for both **ACC 3** and **ACC 4** signatures (p = 0.0019 and 0.0044, respectively) as did COC 2 for **ACC 3** (p = 0.027) (Fig. 4B), suggesting these cell types are predominantly enriched in tumours with comparably good prognosis. No significant difference in scores for **ACC 5** or **ACC M** were found across molecular subtypes. Thus, cellular populations **ACC 1** and **ACC 2**, which are found to characterise group II and group I samples, respectively, are likely overrepresented in the most aggressive ACC molecular subtypes (Zheng et al., 2016).

3.4. Alternative adrenocortical cellular lineages in ACC

We noticed that a majority (68.3%) of cells from ACC samples were annotated as cell types **UZ** or **ZF 1–3** (Fig. 1D), and each have log ROP scores close to zero implying that they are approximately equally represented in NAG and ACC samples (Fig. 1B). This should be contrasted with the estimated average tumour purity value of 0.82 reported for ACC (higher than any other TCGA cancer type apart from chromophobe renal cell carcinoma) (Zheng et al., 2016), which might therefore suggest that a large proportion of cells with a cancer genotype still adopt a normal phenotype. Reliable information on the genomic state of **UZ** and **ZF** cells is not accessible without additional DNA sequencing (Trinh et al., 2022), but to gain insight into their nature in the context of other adrenocortical cell types we performed snRNA-seq-informed trajectory inference using Slingshot (Street et al., 2018) (Materials and Methods). Slingshot was chosen as the only method with a nearly perfect usability score that

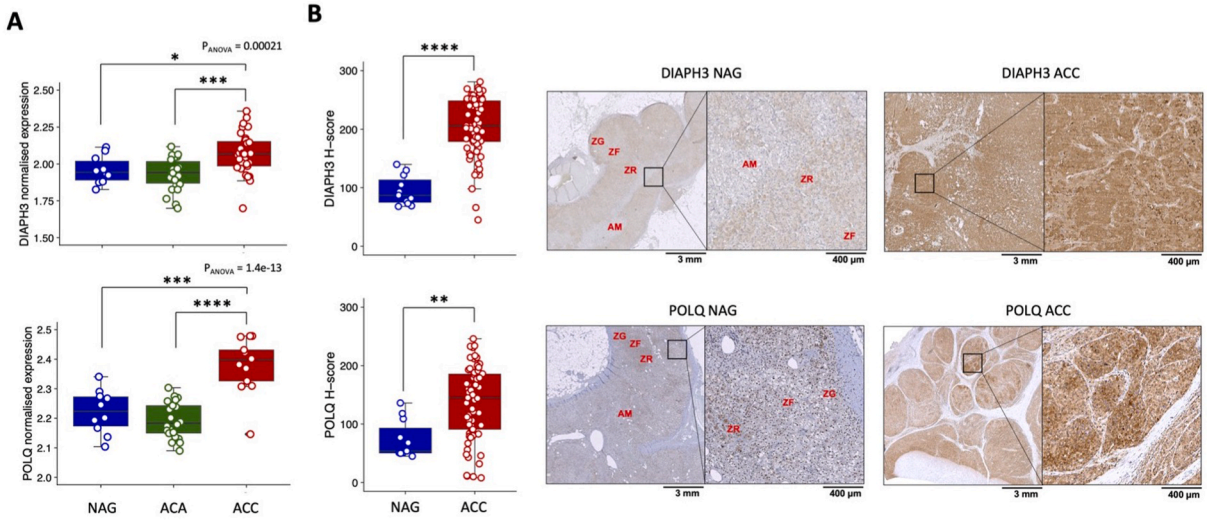

Fig. 3. Validation of top marker genes for ACC M. (A) Summary of *POLQ* and *DIAPH3* expression in bulk RNA from Giordano et al., 2009) (Giordano et al., 2009) with NAG (n = 10), ACA (n = 22) and ACC (n = 33) samples. (B) Validation of *POLQ* and *DIAPH3* expression at protein including representative images from IHC.

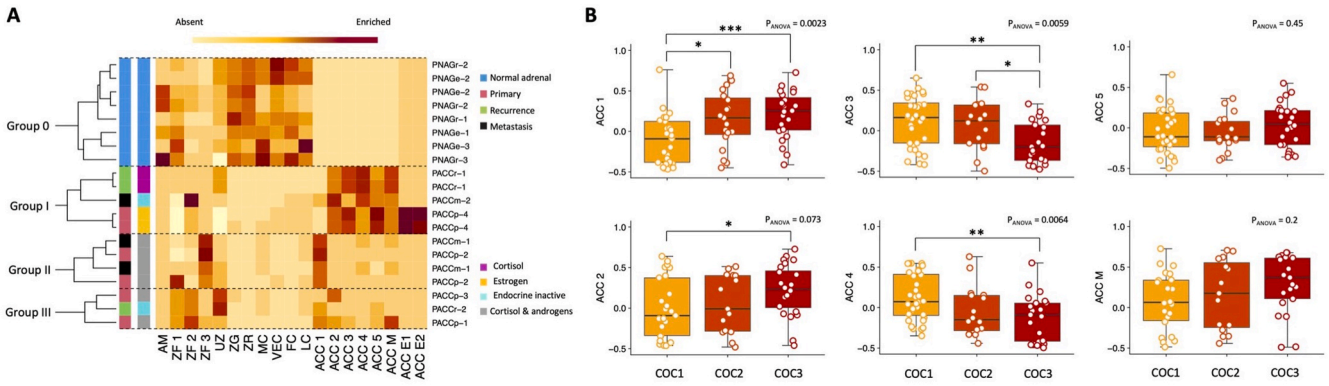

Fig. 4. Grouping of ACC tumours by cellular compositions and molecular subtypes. (A) Heatmap showing the hierarchical clustering of NAG (Group 0) and ACC samples (Groups I, II and III) based on the relative proportions of cell types, coloured with a gradient going from zero (no cells of that type in corresponding sample, white) to one (all cells of that type in corresponding sample, dark red). (B) Scores for the six ACC specific (excludes **ACC E1** and **E2** from estrogen patient PACCp-4) single-cell signatures across TCGA-ACC samples grouped into their molecular subtypes.

performs consistently across a wide range of evaluation criteria (Saelens et al., 2019); it is not fully reliable with disconnected regions in the dimensional reduction however, so we excluded cell types **ACC M**, **ACC E1** and **ACC E2** from trajectory analysis. Slingshot predicted six lineages based on a branched topology that contained branch points at **UZ**, **ZF 1** and **ACC 5** (Fig. S4A). In addition to being enriched for a large number of signalling pathways and proliferative markers, **ACC 5** also scored highest for an adapted version of the StemID score (Grün et al., 2016) (Material and Methods), consequently identifying **ACC 5** as a candidate progenitor cell type for the cellular differentiation lineages obtained by Slingshot (Fig. 5A).

Lineages L1, L2 and L3 are consistent with a centripetal migration and differentiation model of adrenocortical zonation where the ZF progressively matures (as measured by *DLK1* expression; average log2 fold change = 1.09 and 0.97, and adjusted p = 1.51e-153 and adjusted p < 1.51e-153 in **ZF 2** and **ZF 3**, respectively) and the **ZR** emerges from the steroidogenic ZF phenotype (**ZF 1**), while the **ZG** emerges from a progenitor or intermediate cell type (**UZ**) (Chang et al., 2013; Pignatti et al., 2017; Little et al., 2021). Lineages L4 and L5 (terminating in **ACC 1** and **ACC 2**, respectively) also pass through the **UZ** intermediate cell type and have sharply increasing expression of several PDE genes compared to lineages L1 and L2 (terminating in **ZR** and **ZF 3**, respectively), where expression either decreases or remains approximately constant (Fig. 5B). Increased PDE expression along lineages L4 and L5 may lead to a decrease in cAMP levels that blocks differentiation into the ZF or ZR phenotypes, which depends on PKA signalling in healthy adrenocortical tissue (Drelon et al., 2016a; Mathieu et al., 2018; Dumontet et al., 2018). Fig. 5B also displays L1, L2, L4 and L5 lineage scores for three gene sets defined in previous adrenocortical studies: adrenal differentiation score (ADS) from the TCGA-ACC study (Zheng et al., 2016), and the foetal zone (FZ, inner layer involved in early androgen biosynthesis similar to the adult ZR) and definitive zone (DZ, histologically similar to the postnatal ZG and outer ZF) signatures from a recent single-cell study of the developing adrenal gland (del Valle et al., 2023). The scoring patterns for ADS and FZ are closely related and **ZR**, **ZF 2** and **ACC 2** score higher than **ZF 3** and **ACC 1** for these signatures, respectively. Conversely, the scoring pattern is inverted for DZ (**ZF 3** and **ACC 1**, which both express the DZ marker *NOV* (Ratcliffe et al., 2003), score higher than **ZR**, **ZF 2** and **ACC 2** for this signature), and on further inspection we found that a significantly higher proportion of **ZF 3** cells are

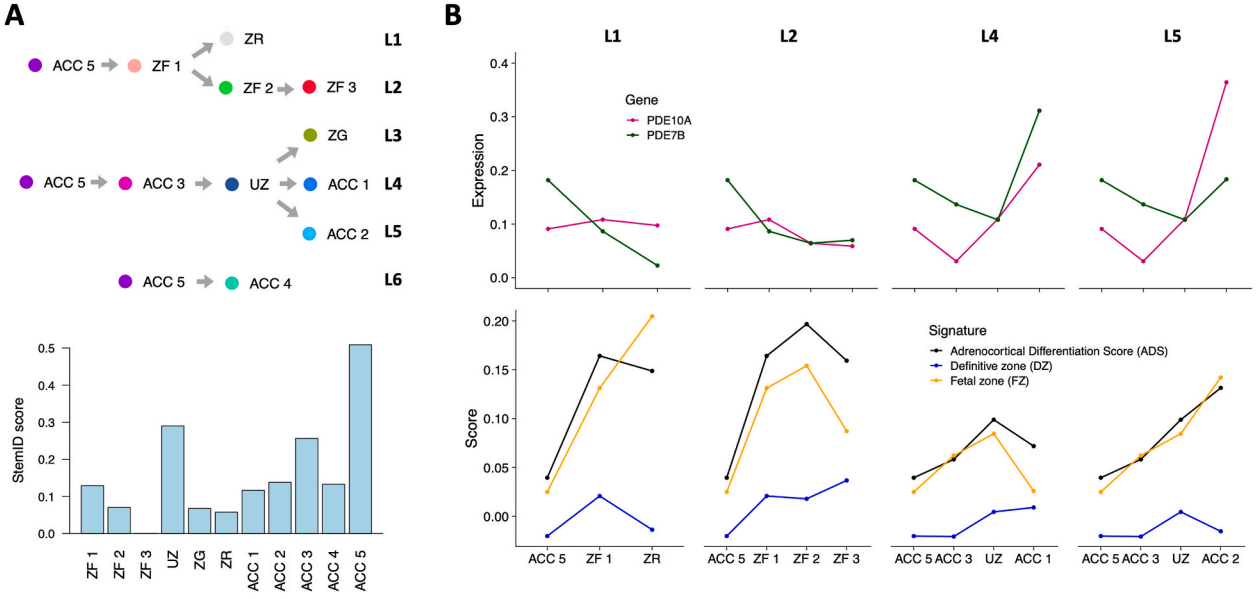

Fig. 5. Adrenocortical lineages in NAG and ACC. (A) Graphical summary of adrenocortical cell types lineages obtained from trajectory inference with **ACC 5** as a root node based on it having the highest StemID score ((Grün et al., 2016) and Materials and Methods) among all included cell types. (B) Expression levels (SCT normalised) across lineages L1, L2, L4 and L5 for *PDE10A* and *PDE7B* (upper four graphs) and scores for published adrenocortical gene sets (lower four graphs).

found in group II samples ($p < 2.2e-16$; 95% CI [20.8%,22.9%] and [19.6%,22.0%] greater than groups I and III, respectively), as observed previously for **ACC 1**. This highlights that group II samples are distinguished, not only by a greater proportion of **ACC 1** cell types, but also by an increased proportion of cells that progress to mature a differentiation phenotype characterised by increased *DLK1* expression along the ZF lineage L2 (Fig. S4B).

3.5. Role of the imprinted DLK1/MEG3 genomic region in adrenocortical cell fate

Alongside imprinted gene *DLK1* that is suspected to play a role in healthy and diseased adrenocortical zonation (Altieri et al., 2022; Hadjidemetriou et al., 2019), imprinted gene *IGF2* is another top marker for cell types **ZF 2** and **ZF 3** at the ends of lineage L2 (average log2 fold change = 1.30 and 0.81, adjusted $p = 6.52e-122$ and adjusted $p < 2.17e-302$, respectively) (Table S1). *IGF2* and *DLK1* are also the two genes most overexpressed (when ranked by average log2 fold change) in ACC compared to NAG tissue comparing within ZF cell types **ZF 1**, **ZF 2** and **ZF 3** (Table S4). The relevance of *IGF2* overexpression in ACC has been the subject of intense investigation (Guillaud-Bataille et al., 2014; V et al., 1993; Soon et al., 2009; Gicquel et al., 2001), and both *IGF2* and *DLK1* are paternally expressed genes encoding signalling ligands expressed within developing adrenal cortex with cognate receptors found on mesenchymal cells of the adrenal capsule (del Valle et al., 2023). We observed that *MEG3*, expressed from the maternal allele at the imprinted *DLK1/MEG3* chromosomal locus 14q32.2, serves as a top marker gene for the **ACC 2** cell type (average log2 fold change = 0.77, adjusted $p < 2.17e-302$) from group I samples, but is not as strongly expressed by the **ACC 1** and **ZF 3** cell types enriched among group II samples (Figs. S3C and S3D and Table S1). We therefore hypothesised that patterns of *DLK1/MEG3* expression across cell types (Fig. S3D) may reflect different underlying genetic alterations at the imprinted 14q32.2 locus, which could potentially explain alternative cellular compositions of different ACC samples. To explore this, we used the top 20 marker gene single-cell signatures for **ACC 1** and **ACC 2** to score TCGA-ACC samples separated by chromosomal copy number state (Steele et al., 2022) of the 14q32.2 region. Strikingly, we found that samples that have undergone chromosomal gains in this region score significantly higher for the **ACC 1** signature ($p = 0.046$) while those that had undergone

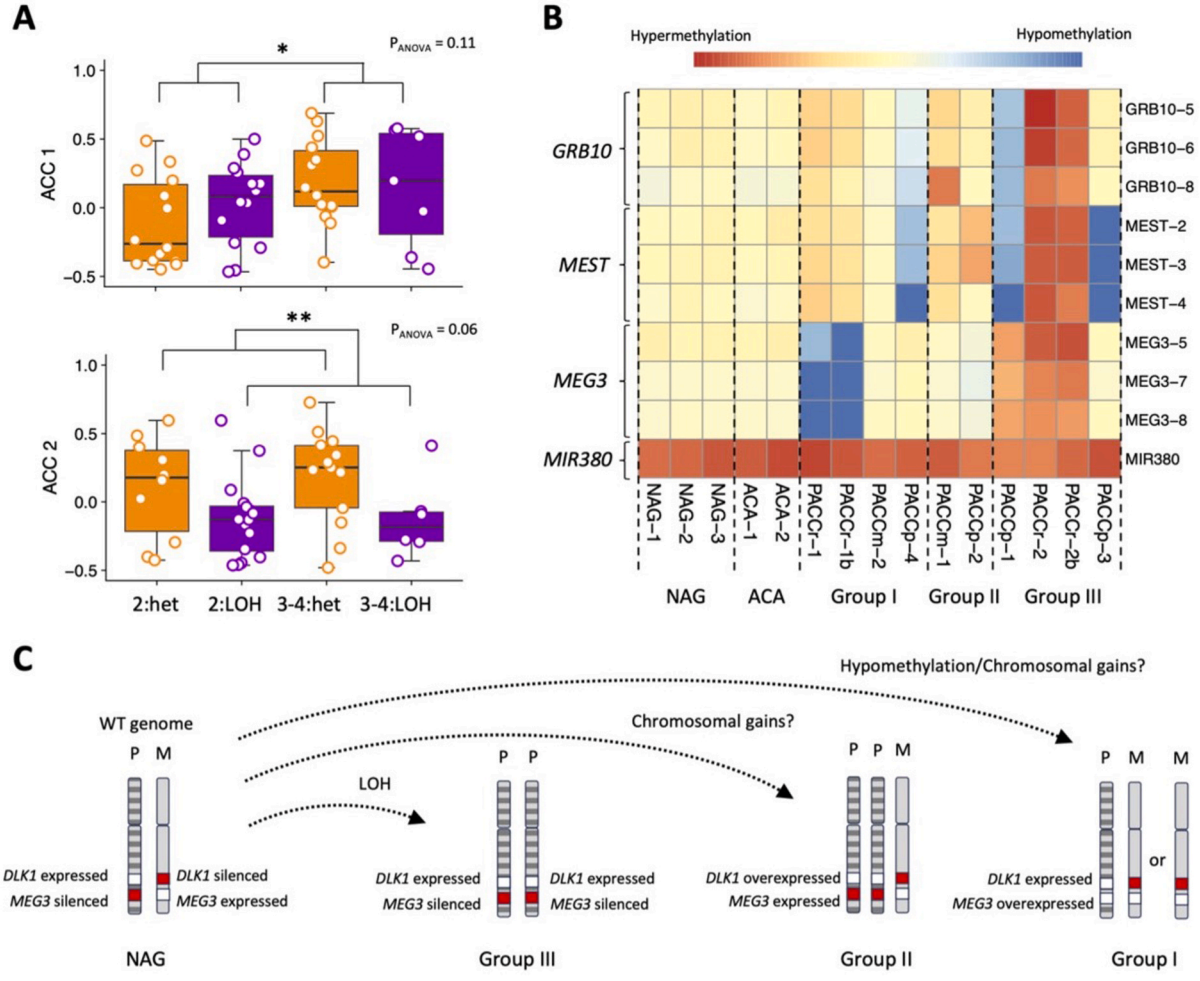

Fig. 6. Associations of cell type compositions with state of imprinted 14q32.2 region. (A) Scores for single-cell signatures **ACC 1** and **ACC 2** across TCGA-ACC samples grouped by copy number state at the 14q32.2 region encoding *DLK1* and *MEG3*. Only copy number segments larger than 40Mbp are included and chromosomal gains of more than four are excluded. Heterozygous segments are those with $A > 0$, $B > 0$ (reflecting the counts for major allele A and minor allele B) while LOH are those with $A > 0$, $B = 0$: diploid wildtype or copy neutral LOH (2:het and 2:LOH, respectively) and chromosomal gains (3–4:het or 3–4:LOH). (B) Heat map showing the methylation status of probed genomic regions in NAG, ACA and ACC samples grouped according to cellular composition. (C) Cartoon schematic illustrating possible mechanisms for generating different ACC cellular compositions based on alterations at the imprinted 14q32.2 region. Group II samples, characterised by enrichment for **ACC 1** and **ZF 3** (*DLK1* high) populations, possibly associated with copy number gains of the parental (P) allele. Loss of methylation at the *MEG3* locus and/or copy number gains of the maternal (M) allele could underlie enrichment of **ACC 2** (*MEG3* high) populations in group I samples, while both **ACC 1** and **ACC 2** cell types are comparatively depleted in group III samples associated with copy neutral LOH.

copy neutral LOH score significantly lower for the **ACC 2** signature ($p = 0.01$) (Fig. 6A).

Finally, to corroborate the relationship between 14q32.2 chromosomal state and ACC cellular composition, we performed MS-MLPA to assess the methylation status of this genomic region (Materials and Methods). In healthy cells, imprinting of 14q32.2 is controlled by methylation of the *MEG3* coding region on the paternal allele, which restricts its expression to the maternal (unmethylated) allele. We first confirmed that MS-MLPA can reliably detect and distinguish hypo-, hyper- and heterozygous methylation states of *MEG3* (and known methylated regions *GRB10*, *MEST*, *MIR380*) using DNA isolated from paired patient blood samples to show these have the same methylation patterns as NAG and ACA controls (Fig. S5). The assay was then repeated using DNA isolated from tumour samples from the eight ACC patients included in our study, revealing that two of the three tumours from group III (PACCp-1 and PACCr-2, confirmed by technical replicate) display hypermethylation of *MEG3* associated with complete loss of expression of this gene from the maternal allele (Fig. 6B). Hypermethylation and silencing of *MEG3* expression can arise via several different mechanisms (including LOH of the maternal allele, Fig. 6C) that are not possible to distinguish using MS-MLPA. However, finding this alteration to occur only within samples from group III is entirely consistent with the characterisation of this group by a relative absence of **ACC 1** and **ACC 2** cellular populations, which are potentially associated with retention or additional gains of the maternal allele (Fig. 6C). Furthermore, *MEG3* methylation is found to be entirely absent in one tumour from group I (patient PACCr-1, confirmed by technical replicate) (Fig. 6B), implying that loss of imprinting at the paternal allele could be one possible mechanism driving *MEG3* overexpression within the **ACC 2** cell type from group I samples (Fig. 6C). Taken together, these results strongly suggest that the copy number state and balance of alleles at the *DLK1/MEG3* 14q32.2 locus are associated with relative cellular compositions of different ACC tumours.

4. Discussion

Our understanding of ACC pathogenesis has increased considerably over the past decade following in-depth characterisations of the molecular processes involved in development, homeostasis and tumorigenesis of the adult adrenal gland (Juhlin et al., 2021; Lerario et al., 2022; Assié et al., 2014; Zheng et al., 2016; Pignatti et al., 2017; Little et al., 2021; Vidal et al., 2016; del Valle et al., 2023; Altieri et al., 2022). In the present study, we contribute to this emerging field by providing a cellular transcriptome atlas of ACC at single-nuclei resolution that complements existing data and reveals a mixture of cell types present within the malignant adrenal cortex. Based on a detailed comparison with tissue from healthy human adrenal gland (Altieri et al., 2022), we find a low amount of immune infiltration confirming that ACC is a "cold" immune infiltrate tumour and consistent with previous reports of high tumour purity values (Zheng et al., 2016; Thorsson et al., 2018; Landwehr et al., 2020). We identify at least eight cell types that are specific to ACC, with two that are highly specific for the rare case of a male patient with excess levels of estrogen. ACC samples from our patient cohort separate into three predominant groups (that mix primary, metastatic, and recurrent tumours) according to their underlying composition of the six remaining ACC specific cell types (**ACC 1–5** and **ACC M**).

ACC sample group II is enriched for cell type **ACC 1** that displays hallmarks of cytoskeletal and cell-matrix remodelling driven by calcium signalling (Janke et al., 2023) in addition to a greater proportion of age-associated, *DLK1* and *IGF2* expressing ZF cells (cell type **ZF 3**). Cell type **ACC 1** is also associated with the most aggressive molecular subtype COC3 (Zheng et al., 2016), suggesting that group II represents tumours with the worst patient outcome. Conversely, ACC sample group I is enriched for cell type **ACC 2** that is associated with both COC2 and COC3 molecular subtypes (Zheng et al., 2016), and displays hallmarks of increased cholesterol uptake, early steroid metabolism and high *MEG3* expression. Cell type **ACC 2** may therefore predominantly account for aberrant steroidogenesis in a subgroup of ACC patients with mixed outcome, including those that are deemed clinically endocrine inactive but still may secrete large quantities of steroid hormone precursors (Arlt et al., 2011; Pereira et al., 2020). ACC samples from group III contained far fewer proportions of **ACC 1** and **ACC 2** cell types than groups I and II. Group III therefore likely represents ACC tumours with comparably better patient outcome since they lack these malignant cell types. **ACC 3** and **ACC 4** cell type signatures, found mainly in group I samples, display hallmarks of increased fatty acid metabolism and hypoxia/glycolysis, respectively, and were also preferentially enriched in less-aggressive, COC1 tumours. One possible explanation for this observation is that metabolic perturbations blocking adrenocortical steroidogenesis can inhibit malignant ACC progression (Raff and Bruder, 2006).

Consistent with existing knowledge on the increased expression of cell division and proliferation markers in ACC (Beuschlein et al., 2015), two remaining ACC specific populations **ACC M** and **ACC 5** both display hallmarks of increased DNA replication and mitotic activity. The more abundant cell type, **ACC M**, is characterised by the top marker genes *DIAPH3*, *POLQ* and *EZH2*. *EZH2* has already been implicated in ACC progression (Tabbal et al., 2019; Drelon et al., 2016b) and adrenocortical cell differentiation (Mathieu et al., 2018), and here we validated that *DIAPH3* and *POLQ* are overexpressed at the protein level and have prognostic potential at the RNA level in ACC. *POLQ* is a known DNA polymerase (Sharief et al., 1999) and *DIAPH3* is a relatively uncharacterised protein that has recently been shown to localise to the centrosome during mitosis (Lau et al., 2021), and proposed as a biomarker for prostate and colorectal cancer (Rong et al., 2021; Huang et al., 2022). Of note, *EZH2*, *DIAPH3*, *POLQ* are among the top marker genes for transit amplifying cells (TACs) in a recent single-cell data set comparing human colorectal polyps with normal tissue (Chen et al., 2021), suggesting that **ACC M** might represent a mitotic phenotype with increased prevalence in the diseased state of many self-renewing tissues such as the colon, intestine and adrenal cortex (Tetteh et al., 2015). In this way, increases in numbers of cells from the **ACC M** TAC-like population could drive an enrichment of malignantly differentiated cell types, such as **ACC 1** and **ACC 2**, which are associated with more aggressive ACC tumours.

ACC 5 was identified as the least abundant ACC specific cell type and is characterised by high scores for WNT, TGF-beta and NOTCH signalling pathways and top marker genes *MIK67*, *LGR4, JAG1, SOX4, NFE2L3* and *NR3C1*. Among these top marker genes, expression of the *RSPO3* receptor *LGR4* was also recently detected in the developing adrenal cortex (del Valle et al., 2023) and its mutation is known to drive aberrant adrenocortical zonation (Lucas et al., 2023). *RSPO3* is itself a WNT signalling coactivator that is proposed to play a key role in maintaining the adrenocortical stem cell niche near the adrenal capsule (Little et al., 2021; Vidal et al., 2016; Basham et al., 2019; Pignatti et al., 2020; del Valle et al., 2023; Altieri et al., 2022). This model is once again analogous to the mechanism for maintenance of the *LGR5*+ (homologue *RSPO3* receptor) stem cell compartment in colon or intestine, whose perturbation during carcinogenesis involves aberrant differentiation of TACs into absorptive or secretory cell types based on levels of NOTCH signalling (Tetteh et al., 2015; Reya and Clevers, 2005; Van Es et al., 2012; Batlle and Clevers, 2017). In further support of this model, we have demonstrated that adrenocortical lineages and cellular compositions of the different ACC sample groups are associated with abnormal copy number states and allelic imbalances of the imprinted 14q32.2 locus, which encodes the non-canonical NOTCH ligand *DLK1* and maternally expressed gene *MEG3*. Silencing of *MEG3* through LOH of the maternal allele could reduce the rate of differentiation into cell types **ACC 1** and **ACC 2**, which are both underrepresented among group III samples and instead associated with more aggressive COC2 and COC3 tumours. This is consistent with previous results that show LOH of the maternal *DLK1/MEG3* allele is ubiquitous across a subset of ACC tumours with comparably favourable outcome (Assié et al., 2014; Cherradi, 2016). While loss of the maternal allele may provide a selective

advantage in early stages of disease (Modali et al., 2015; Zhou et al., 2012; Iyer et al., 2017), this alteration perhaps prevents progression into more advanced stages of ACC.

These data have several limitations, including a relatively small patient cohort due to the restricted availability of biological tissue for such a rare disease and the fact that snRNA-seq as a method can have limited sensitivity at low gene expression levels. The ability to expand single-cell profiling to larger patient cohorts and include more sequencing reads per cell will help to further advance our initial findings and hypotheses. Although knowledge of the molecular sequence of events involved in the pathogenesis of ACC remains far from complete, the present study provides some novel insights into the vast landscape of cells and genes that are involved in this process. Our results therefore constitute an essential contribution to the biological and clinical comprehension of this devastating disease by identifying the malignant cell types associated with prognostic classification. Future work will be required to validate the precise molecular mechanisms that generate cellular and clinical heterogeneity of ACC tumours, which may negatively impact treatment as it does for other cancers (Lenz et al., 2022). In this way, our initial study paves the way for a better understanding of ACC that will ultimately drive identification of new drug targets and therapeutic opportunities.

Data and code availability

Raw sequencing data associated with this study have been uploaded to NIH Sequence Read Archive (SRA) under BioProject accession number PRJNA1024912 accessible via the link http://www.ncbi.nlm.nih.gov/bioproject/1024912. All code for reproducing the analyses presented in this article are freely available at https://gitlab.com/davidtourigny/adrenal-cortical-carcinoma.

CRediT authorship contribution statement

David S. Tourigny: Writing – review & editing, Writing – original draft, Software, Investigation, Formal analysis, Conceptualization. **Barbara Altieri:** Writing – review & editing, Validation, Investigation, Conceptualization. **Kerim A. Secener:** Writing – review & editing, Investigation, Data curation, Conceptualization. **Silviu Sbiera:** Supervision, Project administration. **Marc P. Schauer:** Investigation. **Panagiota Arampatzi:** Investigation. **Sabine Herterich:** Validation, Methodology. **Sascha Sauer:** Supervision, Funding acquisition, Conceptualization. **Martin Fassnacht:** Writing – review & editing, Supervision, Funding acquisition, Conceptualization. **Cristina L. Ronchi:** Writing – review & editing, Supervision, Project administration, Methodology, Investigation, Funding acquisition, Conceptualization.

Declaration of competing interest

The authors declare that they have no known competing financial interests or personal relationships that could have appeared to influence the work reported in this paper.

Data availability

Raw sequencing data associated with this study have been uploaded to NIH Sequence Read Archive (SRA) under BioProject accession number PRJNA1024912.

Acknowledgements

The authors are grateful to Ms. Michaela Haaf for coordinating the clinical data entry in Würzburg of the ENSAT registry. This work has been carried out with the help of the Interdisciplinary Bank of Biomaterials and Data of the University Hospital of Würzburg and the Julius Maximilian University of Würzburg (IBDW). The implementation of the IBDW has been supported by the Federal Ministry for Education and Research (grant number FKZ: 01EY1102). This work has been supported by the Deutsche Forschungsgemeinschaft (DFG) (project FA-466/8–1, RO-5435/3–1 and 405560224 (M.F., C.L.R., and S.S.)) and within the CRC/Transregio (project number: 314061271 – TRR 205), and the Deutsche Krebshilfe (70113526 M.F. and C.L.R.).

Appendix A. Supplementary data

Supplementary data to this article can be found online at https://doi.org/10.1016/j.mce.2024.112272.

References

Altieri, B., Ronchi, C.L., Kroiss, M., Fassnacht, M., 2020. Next-generation therapies for adrenocortical carcinoma. Best Pract. Res. Clin. Endocrinol. Metabol. 34 (3).

Altieri, B., Secener, A.K., Sai, S., Fischer, C., Sbiera, S., Arampatzi, P., Herterich, S., Landwehr, L.S., Vitcetz, S.N., Braeuning, C., Fassnacht, M., Ronchi, C.L., Sauer, S., 2022. Cell atlas at single-nuclei resolution of the adult human adrenal gland and adrenocortical adenomas. bioRxiv 2022. https://doi.org/10.1101/2022.08.27.505530.

Arlt, W., Biehl, M., Taylor, A.E., Hahner, S., Libé, R., Hughes, B.A., Schneider, P., Smith, D.J., Stiekema, H., Krone, N., Porfiri, E., Opocher, G., Bertherat, J., Mantero, F., Allolio, B., Terzolo, M., Nightingale, P., Shackleton, C.H.L., Bertagna, X., Fassnacht, M., Stewart, P.M., 2011. Urine steroid Metabolomics as a biomarker tool for detecting malignancy in adrenal tumors. J. Clin. Endocrinol. Metab. 96 (12), 3775.

Assié, G., Letouzé, E., Fassnacht, M., Jouinot, A., Luscap, W., Barreau, O., Omeiri, H., Rodriguez, S., Perlemoine, K., René-Corail, F., Elarouci, N., Sbiera, S., Kroiss, M., Allolio, B., Waldmann, J., Quinkler, M., Mannelli, M., Mantero, F., Papathomas, T., De Krijger, R., Tabarin, A., Kerlan, V., Baudin, E., Tissier, F., Dousset, B., Groussin, L., Amar, L., Clauser, E., Bertagna, X., Ragazzon, B., Beuschlein, F., Libé, R., De Reyniès, A., Bertherat, J., 2014. Integrated genomic characterization of adrenocortical carcinoma. Nat. Genet. 46 (6), 607–612.

Baron, M., Veres, A., Wolock, S.L., Faust, A.L., Gaujoux, R., Vetere, A., Ryu, J.H., Wagner, B.K., Shen-Orr, S.S., Klein, A.M., Melton, D.A., Yanai, I., 2016. A single-cell transcriptomic map of the human and mouse pancreas reveals inter- and intra-cell population structure. Cell Syst. 3 (4), 346–360.e4.

Basham, K.J., Rodriguez, S., Turcu, A.F., Lerario, A.M., Logan, C.Y., Rysztak, M.R., Gomez-Sanchez, C.E., Breault, D.T., Koo, B.K., Clevers, H., Nusse, R., Val, P., Hammer, G.D., 2019. A ZNRF3-dependent Wnt/β-catenin signaling gradient is required for adrenal homeostasis. Genes Dev. 33 (3–4), 209–220.

Batlle, E., Clevers, H., 2017. Cancer stem cells revisited. Nat. Med. 23 (10), 1124–1134.

Beuschlein, F., Weigel, J., Saeger, W., Kroiss, M., Wild, V., Daffara, F., Libé, R., Ardito, A., Ghuzlan, A Al, Quinkler, M., Oßwald, A., Ronchi, C.L., De Krijger, R., Feelders, R.A., Waldmann, J., Willenberg, H.S., Deutschbein, T., Stell, A., Reincke, M., Papotti, M., Baudin, E., Tissier, F., Haak, H.R., Loli, P., Terzolo, M., Allolio, B., Müller, H.H., Fassnacht, M., 2015. Major prognostic role of Ki67 in localized adrenocortical carcinoma after complete resection. J. Clin. Endocrinol. Metab. 100 (3), 841–849.

Butler, A., Hoffman, P., Smibert, P., Papalexi, E., Satija, R., 2018. Integrating single-cell transcriptomic data across different conditions, technologies, and species. Nat. Biotechnol. 36 (5), 411–420.

Chang, S.P., Morrison, H.D., Nilsson, F., Kenyon, C.J., West, J.D., Morley, S.D., 2013. Cell proliferation, movement and differentiation during maintenance of the adult mouse adrenal cortex. PLoS One 8 (12), e81865.

Chen, B., Scurrah, C.R., McKinley, E.T., Simmons, A.J., Ramirez-Solano, M.A., Zhu, X., Markham, N.O., Heiser, C.N., Vega, P.N., Rolong, A., Kim, H., Sheng, Q., Drewes, J. L., Zhou, Y., Southard-Smith, A.N., Xu, Y., Ro, J., Jones, A.L., Revetta, F., Berry, L.D., Niitsu, H., Islam, M., Pelka, K., Hofree, M., Chen, J.H., Sarkizova, S., Ng, K., Giannakis, M., Boland, G.M., Aguirre, A.J., Anderson, A.C., Rozenblatt-Rosen, O., Regev, A., Hacohen, N., Kawasaki, K., Sato, T., Goettel, J.A., Grady, W.M., Zheng, W., Washington, M.K., Cai, Q., Sears, C.L., Goldenring, J.R., Franklin, J.L., Su, T., Huh, W.J., Vandekar, S., Roland, J.T., Liu, Q., Coffey, R.J., Shrubsole, M.J., Lau, K.S., 2021. Differential pre-malignant programs and microenvironment chart distinct paths to malignancy in human colorectal polyps. Cell 184 (26), 6262–6280.e26.

Cherradi, N., 2016. microRNAs as potential biomarkers in adrenocortical cancer: progress and challenges. Front. Endocrinol. 6 (JAN).

del Valle, I., Young, M.D., Kildisiute, G., Ogunbiyi, O.K., Buonocore, F., Simcock, I.C., Khabirova, E., Crespo, B., Moreno, N., Brooks, T., Niola, P., Swarbrick, K., Suntharalingham, J.P., McGlacken-Byrne, S.M., Arthurs, O.J., Behjati, S., Achermann, J.C., 2023. An integrated single-cell analysis of human adrenal cortex development. JCI Insight 8 (14).

Detomas, M., Altieri, B., Schlötelburg, W., Appenzeller, S., Schlaffer, S., Coras, R., Schirbel, A., Wild, V., Kroiss, M., Sbiera, S., Fassnacht, M., Deutschbein, T., 2021. Case report: consecutive adrenal cushing's syndrome and cushing's disease in a patient with somatic CTNNB1, USP8, and NR3C1 mutations. Front. Endocrinol. 12.

Di, Dalmazi G., Altieri, B., Scholz, C., Sbiera, S., Luconi, M., Waldman, J., Kastelan, D., Ceccato, F., Chiodini, I., Arnaldi, G., Riester, A., Osswald, A., Beuschlein, F., Sauer, S., Fassnacht, M., Appenzeller, S., Ronchi, C.L., 2020. RNA sequencing and somatic mutation status of adrenocortical tumors: novel pathogenetic insights. J. Clin. Endocrinol. Metab. 105 (12).

Drelon, C., Berthon, A., Sahut-Barnola, I., Mathieu, M., Dumontet, T., Rodriguez, S., Batisse-Lignier, M., Tabbal, H., Tauveron, I., Lefrançois-Martinez, A.M., Pointud, J. C., Gomez-Sanchez, C.E., Vainio, S., Shan, J., Sacco, S., Schedl, A., Stratakis, C.A., Martinez, A., Val, P., 2016a. PKA inhibits WNT signalling in adrenal cortex zonation and prevents malignant tumour development. Nat. Commun. 7.

Drelon, C., Berthon, A., Mathieu, M., Ragazzon, B., Kuick, R., Tabbal, H., Septier, A., Rodriguez, S., Batisse-Lignier, M., Sahut-Barnola, I., Dumontet, T., Pointud, J.C., Lefrançois-Martinez, A.M., Baron, S., Giordano, T.J., Bertherat, J., Martinez, A., Val, P., 2016b. EZH2 is overexpressed in adrenocortical carcinoma and is associated with disease progression. Hum. Mol. Genet. 25 (13), 2789.

Dumontet, T., Sahut-Barnola, I., Septier, A., Montanier, N., Plotton, I., Roucher-Boulez, F., Ducros, V., Lefrançois-Martinez, A.M., Pointud, J.C., Zubair, M., Morohashi, K.I., Breault, D.T., Val, P., Martinez, A., 2018. PKA signaling drives reticularis differentiation and sexually dimorphic adrenal cortex renewal. JCI insight 3 (2).

Fassnacht, M., Dekkers, O.M., Else, T., Baudin, E., Berruti, A., De Krijger, R.R., Haak, H. R., Mihai, R., Assie, G., Terzolo, M., 2018. European society of endocrinology clinical practice guidelines on the management of adrenocortical carcinoma in adults, in collaboration with the European network for the study of adrenal tumors. Eur. J. Endocrinol. 179 (4), G1–G46.

Fojo, T., Huff, L., Litman, T., Im, K., Edgerly, M., del Rivero, J., Pittaluga, S., Merino, M., Bates, S.E., Dean, M., 2020. Metastatic and recurrent adrenocortical cancer is not defined by its genomic landscape. BMC Med. Genom. 13 (1).

Gara, S.K., Lack, J., Zhang, L., Harris, E., Cam, M., Kebebew, E., 2018. Metastatic adrenocortical carcinoma displays higher mutation rate and tumor heterogeneity than primary tumors. Nat. Commun. 9 (1).

Gicquel, C., Bertagna, X., Gaston, V., Coste, J., Louvel, A., Baudin, E., Bertherat, J., Chapuis, Y., Duclos, J.M., Schlumberger, M., Plouin, P.F., Luton, J.P., Le Bouc, Y., 2001. Molecular markers and long-term recurrences in a large cohort of patients with sporadic adrenocortical tumors. Cancer Res. 61 (18), 6762–6767.

Giordano, T.J., Kuick, R., Else, T., Gauger, P.G., Vinco, M., Bauersfeld, J., Sanders, D., Thomas, D.G., Doherty, G., Hammer, G., 2009. Molecular classification and prognostication of adrenocortical tumors by transcriptome profiling. Clin. Cancer Res. 15 (2), 668–676.

Glinka, A., Dolde, C., Kirsch, N., Huang, Y.L., Kazanskaya, O., Ingelfinger, D., Boutros, M., Cruciat, C.M., Niehrs, C., 2011. LGR4 and LGR5 are R-spondin receptors mediating Wnt/β-catenin and Wnt/PCP signalling. EMBO Rep. 12 (10), 1055.

Grün, D., Muraro, M.J., Boisset, J.C., Wiebrands, K., Lyubimova, A., Dharmadhikari, G., van den Born, M., van Es, J., Jansen, E., Clevers, H., de Koning, E.J.P., van Oudenaarden, A., 2016. De Novo prediction of stem cell identity using single-cell transcriptome data. Cell Stem Cell 19 (2), 266.

Guillaud-Bataille, M., Ragazzon, B., De Reyniès, A., Chevalier, C., Francillard, I., Barreau, O., Steunou, V., Guillemot, J., Tissier, F., Rizk-Rabin, M., René-Corail, F., Al Ghuzlan, A., Assié, G., Bertagna, X., Baudin, E., Le Bouc, Y., Bertherat, J., Clauser, E., 2014. IGF2 promotes growth of adrenocortical carcinoma cells, but its overexpression does not modify phenotypic and molecular features of adrenocortical carcinoma. PLoS One 9 (8).

Hadjidemetriou, I., Mariniello, K., Ruiz-Babot, G., Pittaway, J., Mancini, A., Mariannis, D., Gomez-Sanchez, C.E., Parvanta, L., Drake, W.M., Chung, T.T., Abdel-Aziz, T.E., DiMarco, A., Palazzo, F.F., Wierman, M.E., Kiseljak-Vassiliades, K., King, P.J., Guasti, L., 2019. DLK1/PREF1 marks a novel cell population in the human adrenal cortex. J. Steroid Biochem. Mol. Biol. 193, 105422.

Hänzelmann, S., Castelo, R., Guinney, J., 2013. GSVA: gene set variation analysis for microarray and RNA-seq data. BMC Bioinf. 14.

Hashimshony, T., Senderovich, N., Avital, G., Klochendler, A., de Leeuw, Y., Anavy, L., Gennert, D., Li, S., Livak, K.J., Rozenblatt-Rosen, O., Dor, Y., Regev, A., Yanai, I., 2016. CEL-Seq2: sensitive highly-multiplexed single-cell RNA-Seq. Genome Biol. 17 (1), 1–7.

Hollenberg, S.M., Weinberger, C., Ong, E.S., Cerelli, G., Oro, A., Lebo, R., Brad Thompson, E., Rosenfeld, M.G., Evans, R.M., 1985. Primary structure and expression of a functional human glucocorticoid receptor cDNA. Nature 318 (6047), 635–641.

Huang, R., Wu, C., Wen, J., Yu, J., Zhu, H., Yu, J., Zou, Z., 2022. DIAPH3 is a prognostic biomarker and inhibit colorectal cancer progression through maintaining EGFR degradation. Cancer Med. 11 (23), 4688–4702.

Iyer, S., Modali, S.D., Agarwal, S.K., 2017. Long noncoding RNA MEG3 is an epigenetic determinant of oncogenic signaling in functional pancreatic neuroendocrine tumor cells. Mol. Cell Biol. 37 (22).

Janke, E.K., Chalmers, S.B., Roberts-Thomson, S.J., Monteith, G.R., 2023. Intersection between calcium signalling and epithelial-mesenchymal plasticity in the context of cancer. Cell Calcium 112.

Juhlin, C.C., Bertherat, J., Giordano, T.J., Hammer, G.D., Sasano, H., Mete, O., 2021. What did we learn from the molecular biology of adrenal cortical neoplasia? From histopathology to translational genomics. Endocr. Pathol. 32 (1), 102–133.

Kim, J.H., Choi, M.H., 2020. Embryonic development and adult regeneration of the adrenal gland. Endocrinol. Metab. 35 (4), 765.

Krishnaswami, S.R., Grindberg, R.V., Novotny, M., Venepally, P., Lacar, B., Bhutani, K., Linker, S.B., Pham, S., Erwin, J.A., Miller, J.A., Hodge, R., McCarthy, J.K., Kelder, M., McCorrison, J., Aevermann, B.D., Fuertes, F.D., Scheuermann, R.H., Lee, J., Lein, E.S., Schork, N., McConnell, M.J., Gage, F.H., Lasken, R.S., 2016. Using single nuclei for RNA-seq to capture the transcriptome of postmortem neurons. Nat. Protoc. 11 (3), 499–524, 113. 2016 Feb 18.

Landwehr, L.S., Altieri, B., Schreiner, J., Sbiera, I., Weigand, I., Kroiss, M., Fassnacht, M., Sbiera, S., 2020. Interplay between glucocorticoids and tumor-infiltrating lymphocytes on the prognosis of adrenocortical carcinoma. J. Immunother Cancer 8 (1).

Lau, E.O.C., Damiani, D., Chehade, G., Ruiz-Reig, N., Saade, R., Jossin, Y., Aittaleb, M., Schakman, O., Tajeddine, N., Gailly, P., Tissir, F., 2021. DIAPH3 deficiency links microtubules to mitotic errors, defective neurogenesis, and brain dysfunction. Elife 10.

Lenz, G., Onzi, G.R., Lenz, L.S., Buss, J.H., dos Santos, J.A., Begnini, K.R., 2022. The origins of phenotypic heterogeneity in cancer. Cancer Res. 82 (1), 3–11.

Lerario, A.M., Mohan, D.R., Hammer, G.D., 2022. Update on biology and genomics of adrenocortical carcinomas: rationale for emerging therapies. Endocr. Rev. 43 (6), 1051–1073.

Li, L., Krantz, I.D., Deng, Y., Genin, A., Banta, A.B., Collins, C.C., Qi, M., Trask, B.J., Kuo, W.L., Cochran, J., Costa, T., Pierpont, M.E.M., Rand, E.B., Piccoli, D.A., Hood, L., Spinner, N.B., 1997. Alagille syndrome is caused by mutations in human Jagged1, which encodes a ligand for Notch1. Nat. Genet. 16 (3), 243–251.

Libé, R., 2019. Clinical and molecular prognostic factors in adrenocortical carcinoma. Minerva Endocrinol. 44 (1), 58–69.

Lippert, J., Dischinger, U., Appenzeller, S., Prete, A., Kircher, S., Skordilis, K., Elhassan, Y.S., Altieri, B., Fassnacht, M., Ronchi, C.L., 2023. Performance of DNA-based biomarkers for classification of adrenocortical carcinoma: a prognostic study. Eur. J. Endocrinol. 189 (2), 262–270.

Little, D.W., Dumontet, T., LaPensee, C.R., Hammer, G.D., 2021. β-catenin in adrenal zonation and disease. Mol. Cell. Endocrinol. 522.

Lloyd, R.V., Osamura, R.Y., Klöppel, G., Rosai, J., 2017. In: Lloyd, R.V., Osamura, R.Y., Klöppel, G., Rosai, J. (Eds.), WHO Classification of Tumours of Endocrine Organs. International Agency for Research on Cancer, p. 355.

Lucas, C., Sauter, K.S., Steigert, M., Mallet, D., Wilmouth, J., Olabe, J., Plotton, I., Morel, Y., Aeberli, D., Wagner, F., Clevers, H., Pandey, A.V., Val, P., Roucher-Boulez, F., Flück, C.E., 2023. Loss of LGR4/GPR48 causes severe neonatal salt wasting due to disrupted WNT signaling altering adrenal zonation. J. Clin. Invest. 133 (4).

Mathieu, M., Drelon, C., Rodriguez, S., Tabbal, H., Septier, A., Damon-Soubeyrand, C., Dumontet, T., Berthon, A., Sahut-Barnola, I., Djari, C., Batisse-Lignier, M., Pointud, J.C., Richard, D., Kerdivel, G., Calméjane, M.A., Boeva, V., Tauveron, I., Lefrançois-Martinez, A.M., Martinez, A., Val, P., 2018. Steroidogenic differentiation and PKA signaling are programmed by histone methyltransferase EZH2 in the adrenal cortex. Proc. Natl. Acad. Sci. U. S. A. 115 (52), E12265–E12274.

Mete, O., Gucer, H., Kefeli, M., Asa, S.L., 2018. Diagnostic and prognostic biomarkers of adrenal cortical carcinoma. Am. J. Surg. Pathol. 42 (2), 201–213.

Mete, O., Erickson, L.A., Juhlin, C.C., de Krijger, R.R., Sasano, H., Volante, M., Papotti, M.G., 2022. Overview of the 2022 WHO classification of adrenal cortical tumors. Endocr. Pathol. 33 (1), 155–196.

Modali, S.D., Parekh, V.I., Kebebew, E., Agarwal, S.K., 2015. Epigenetic regulation of the lncRNA MEG3 and its target c-MET in pancreatic neuroendocrine tumors. Mol. Endocrinol. 29 (2), 224–237.

Oliveira, S., Pereira, S.S., Costa, M.M., Monteiro, M.P., Pignatelli, D., 2022. Ang-tie angiogenic pathway is distinctively expressed in benign and malignant adrenocortical tumors. Int. J. Mol. Sci. 23 (10).

Papathomas, T.G., Pucci, E., Giordano, T.J., Lu, H., Duregon, E., Volante, M., Papotti, M., Lloyd, R.V., Tischler, A.S., Van Nederveen, F.H., Nose, V., Erickson, L., Mete, O., Asa, S.L., Turchini, J., Gill, A.J., Matias-Guiu, X., Skordilis, K., Stephenson, T.J., Tissier, F., Feelders, R.A., Smid, M., Nigg, A., Korpershoek, E., Van Der Spek, P.J., Dinjens, W.N.M., Stubbs, A.P., De Krijger, R.R., 2016. An international Ki67 reproducibility study in adrenal cortical carcinoma. Am. J. Surg. Pathol. 40 (4), 569–576.

Parekh, S., Ziegenhain, C., Vieth, B., Enard, W., Hellmann, I., 2018. zUMIs - a fast and flexible pipeline to process RNA sequencing data with UMIs. GigaScience 7 (6).

Penny, M.K., Finco, I., Hammer, G.D., 2017. Cell signaling pathways in the adrenal cortex: links tostem/progenitor biology and neoplasia. Mol. Cell. Endocrinol. 445, 42.

Pereira, S.S., Costa, M.M., Gomez-Sanchez, C.E., Monteiro, M.P., Pignatelli, D., 2020. Incomplete pattern of steroidogenic protein expression in functioning adrenocortical carcinomas. Biomedicines 8 (8).

Pignatti, E., Leng, S., Carlone, D.L., Breault, D.T., 2017. Regulation of zonation and homeostasis in the adrenal cortex. Mol. Cell. Endocrinol. 441, 146.

Pignatti, E., Leng, S., Yuchi, Y., Borges, K.S., Guagliardo, N.A., Shah, M.S., Ruiz-Babot, G., Kariyawasam, D., Taketo, M.M., Miao, J., Barrett, P.Q., Carlone, D.L., Breault, D.T., 2020. Beta-catenin causes adrenal hyperplasia by blocking zonal transdifferentiation. Cell Rep. 31 (3).

Raff, H., Bruder, E.D., 2006. Steroidogenesis in human aldosterone-secreting adenomas and adrenal hyperplasias: effects of hypoxia in vitro. Am. J. Physiol. Endocrinol. Metab. 290 (1), 199–203.

Ratcliffe, J., Nakanishi, M., Jaffe, R.B., 2003. Identification of definitive and fetal zone markers in the human fetal adrenal gland reveals putative developmental genes. J. Clin. Endocrinol. Metab. 88 (7), 3272–3277.

Reya, T., Clevers, H., 2005. Wnt signalling in stem cells and cancer. Nature 434 (7035), 843–850.

Rong, Y., Gao, J., Kuang, T., Chen, J., Li, J ang, Huang, Y., Xin, H., Fang, Y., Han, X., Sun, L.Q., Deng, Y.Z., Li, Z., Lou, W., 2021. DIAPH3 promotes pancreatic cancer progression by activating selenoprotein TrxR1-mediated antioxidant effects. J. Cell Mol. Med. 25 (4), 2163.

Saelens, W., Cannoodt, R., Todorov, H., Saeys, Y., 2019. A comparison of single-cell trajectory inference methods. Nat. Biotechnol. 37 (5), 547–554, 375. 2019 Apr 1.

Saliba, J., Coutaud, B., Makhani, K., Epstein Roth, N., Jackson, J., Park, J.Y., Gagnon, N., Costa, P., Jeyakumar, T., Bury, M., Beauchemin, N., Mann, K.K., Blank, V., 2022. Loss of NFE2L3 protects against inflammation-induced colorectal cancer through modulation of the tumor microenvironment. Oncogene 41 (11), 1563–1575.

Sbiera, S., Schmull, S., Assie, G., Voelker, H.U., Kraus, L., Beyer, M., Ragazzon, B., Beuschlein, F., Willenberg, H.S., Hahner, S., Saeger, W., Bertherat, J., Allolio, B., Fassnacht, M., 2010. High diagnostic and prognostic value of steroidogenic factor-1 expression in adrenal tumors. J. Clin. Endocrinol. Metab. 95 (10).

Sbiera, I., Kircher, S., Altieri, B., Fassnacht, M., Kroiss, M., Sbiera, S., 2021. Epithelial and mesenchymal markers in adrenocortical tissues: how mesenchymal are adrenocortical tissues? Cancers 13 (7), 1736.

Sharief, F.S., Vojta, P.J., Ropp, P.A., Copeland, W.C., 1999. Cloning and chromosomal mapping of the human DNA polymerase theta (POLQ), the eighth human DNA polymerase. Genomics 59 (1), 90–96.

Soon, P.S.H., Gill, A.J., Benn, D.E., Clarkson, A., Robinson, B.G., McDonald, K.L., Sidhu, S.B., 2009. Microarray gene expression and immunohistochemistry analyses of adrenocortical tumors identify IGF2 and Ki-67 as useful in differentiating carcinomas from adenomas. Endocr. Relat. Cancer 16 (2), 573–583.

Steele, C.D., Abbasi, A., Islam, S.M.A., Bowes, A.L., Khandekar, A., Haase, K., Hames-Fathi, S., Ajayi, D., Verfaillie, A., Dhami, P., McLatchie, A., Lechner, M., Light, N., Shlien, A., Malkin, D., Feber, A., Proszek, P., Lesluyes, T., Mertens, F., Flanagan, A. M., Tarabichi, M., Van Loo, P., Alexandrov, L.B., Pillay, N., 2022. Signatures of copy number alterations in human cancer. Nature 606 (7916), 984–991.

Street, K., Risso, D., Fletcher, R.B., Das, D., Ngai, J., Yosef, N., Purdom, E., Dudoit, S., 2018. Slingshot: cell lineage and pseudotime inference for single-cell transcriptomics. BMC Genom. 19 (1).

Tabbal, H., Septier, A., Mathieu, M., Drelon, C., Rodriguez, S., Djari, C., Batisse-Lignier, M., Tauveron, I., Pointud, J.C., Sahut-Barnola, I., Ragazzon, B., Assié, G., Bertherat, J., Lefrançois-Martinez, A.M., Martinez, A., Val, P., 2019. EZH2 cooperates with E2F1 to stimulate expression of genes involved in adrenocortical carcinoma aggressiveness. Br. J. Cancer 121 (5), 384.

Tetteh, P.W., Farin, H.F., Clevers, H., 2015. Plasticity within stem cell hierarchies in mammalian epithelia. Trends Cell Biol. 25 (2), 100–108.

Thorsson, V., Gibbs, D.L., Brown, S.D., Wolf, D., Bortone, D.S., Ou Yang, T.H., Porta-Pardo, E., Gao, G.F., Plaisier, C.L., Eddy, J.A., Ziv, E., Culhane, A.C., Paull, E.O., Sivakumar, I.K.A., Gentles, A.J., Malhotra, R., Farshidfar, F., Colaprico, A., Parker, J. S., Mose, L.E., Vo, N.S., Liu, J., Liu, Y., Rader, J., Dhankani, V., Reynolds, S.M., Bowlby, R., Califano, A., Cherniack, A.D., Anastassiou, D., Bedognetti, D., Rao, A., Chen, K., Krasnitz, A., Hu, H., Malta, T.M., Noushmehr, H., Pedamallu, C.S., Bullman, S., Ojesina, A.I., Lamb, A., Zhou, W., Shen, H., Choueiri, T.K., Weinstein, J. N., Guinney, J., Saltz, J., Holt, R., Rabkin, C.E., Caesar-Johnson, S.J., Demchok, J.A., Felau, I., Kasapi, M., Ferguson, M.L., Hutter, C.M., Sofia, H.J., Tarnuzzer, R., Wang, Z., Yang, L., Zenklusen, J.C., Zhang, J., JuliaChudamani, S., Liu, J., Lolla, L., Naresh, R., Pihl, T., Sun, Q., Wan, Y., Wu, Y., Cho, J., DeFreitas, T., Frazer, S., Gehlenborg, N., Getz, G., Heiman, D.I., Kim, J., Lawrence, M.S., Lin, P., Meier, S., Noble, M.S., Saksena, G., Voet, D., Zhang, H., Bernard, B., Chambwe, N., Dhankani, V., Knijnenburg, T., Kramer, R., Leinonen, K., Liu, Y., Miller, M., Reynolds, S., Shmulevich, I., Thorsson, V., Zhang, W., Akbani, R., Broom, B.M., Hegde, A.M., Ju, Z., Kanchi, R.S., Korkut, A., Li, J., Liang, H., Ling, S., Liu, W., Lu, Y., Mills, G.B., Ng, K.S., Rao, A., Ryan, M., Wang, J., Zhang, J., Abeshouse, A., Armenia, J., Chakravarty, D., Chatila, W.K., de Bruijn, I., Gao, J., Gross, B.E., Heins, Z.J., Kundra, R., La, K., Ladanyi, M., Luna, A., Nissan, M.G., Ochoa, A., Phillips, S.M., Reznik, E., Sanchez-Vega, F., Sander, C., Schultz, N., Sheridan, R., Sumer, S.O., Sun, Y., Taylor, B.S., Wang, J., Zhang, H., Anur, P., Peto, M., Spellman, P., Benz, C., Stuart, J.M., Wong, C.K., Yau, C., Hayes, D.N., Parker, J.S., Wilkerson, M.D., Ally, A., Balasundaram, M., Bowlby, R., Brooks, D., Carlsen, R., Chuah, E., Dhalla, N., Jones, S.J.M., Kasaian, K., Lee, D., Ma, Y., Marra, M.A., Mayo, M., Moore, R.A., Mungall, A.J., Mungall, K., Robertson, A.G., Sadeghi, S., Schein, J.E., Sipahimalani, P., Tam, A., Thiessen, N., Tse, K., Wong, T., Berger, A.C., Beroukhim, R., Cibulskis, C., Gabriel, S.B., Ha, G., Meyerson, M., Schumacher, S.E., Shih, J., Kucherlapati, M.H., Kucherlapati, R.S., Baylin, S., Cope, L., Danilova, L., Bootwalla, M.S., Lai, P.H., Maglinte, D.T., Van Den Berg, D.J., Weisenberger, D.J., Auman, J.T., Balu, S., Bodenheimer, T., Fan, C., Hoadley, K.A., Hoyle, A.P., Jefferys, S.R., Jones, C.D., Meng, S., Mieczkowski, P.A., Mose, L.E., Perou, A.H., Perou, C.M., Roach, J., Shi, Y., Simons, J.V., Skelly, T., Soloway, M.G., Tan, D., Veluvolu, U., Fan, H., Hinoue, T., Laird, P.W., Shen, H., Zhou, W., Bellair, M., Chang, K., Covington, K., Creighton, C.J., Dinh, H., Doddapaneni, H.V., Donehower, L.A., Drummond, J., Gibbs, R.A., Glenn, R., Hale, W., Han, Y., Hu, J., Korchina, V., Lee, S., Lewis, L., Li, W., Liu, X., Morgan, M., Morton, D., Muzny, D., Santibanez, J., Sheth, M., Shinbrot, E., Wang, L., Wang, M., Wheeler, D.A., Xi, L., Zhao, F., Hess, J., Appelbaum, E.L., Bailey, M., Cordes, M.G., Ding, L., Fronick, C.C., Fulton, L.A., Fulton, R.S., Kandoth, C., Mardis, E.R., McLellan, M.D., Miller, C.A., Schmidt, H.K., Wilson, R.K., Crain, D., Curley, E., Gardner, J., Lau, K., Mallery, D., Morris, S., Paulauskis, J., Penny, R., Shelton, C., Shelton, T., Sherman, M., Thompson, E., Yena, P., Bowen, J., Gastier-Foster, J.M., Gerken, M., Leraas, K.M., Lichtenberg, T.M., Ramirez, N.C., Wise, L., Zmuda, E., Corcoran, N., Costello, T., Hovens, C., Carvalho, A.L., de Carvalho, A.C., Fregnani, J.H., Longatto-Filho, A., Reis, R.M., Scapulatempo-Neto, C., Silveira, H.C.S., Vidal, D.O., Burnette, A., Eschbacher, J., Hermes, B., Noss, A., Singh, R., Anderson, M.L., Castro, P.D., Ittmann, M., Huntsman, D., Kohl, B., Le, X., Thorp, R., Andry, C., Duffy, E.R., Lyadov, V., Paklina, O., Setdikova, G., Shabunin, A., Tavobilov, M., McPherson, C., Warnick, R., Berkowitz, R., Cramer, D., Feltmate, C., Horowitz, N., Kibel, A., Muto, M., Raut, C.P., Malykh, A., Barnholtz-Sloan, J.S., Barrett, W., Devine, K., Fulop, J., Ostrom, Q.T., Shimmel, K., Wolinsky, Y., Sloan, A.E., De Rose, A., Giuliante, F., Goodman, M., Karlan, B.Y., Hagedorn, C.H., Eckman, J., Harr, J., Myers, J., Tucker, K., Zach, L.A., Deyarmin, B., Hu, H., Kvecher, L., Larson, C., Mural, R.J., Somiari, S., Vicha, A., Zelinka, T., Bennett, J., Iacocca, M., Rabeno, B., Swanson, P., Latour, M., Lacombe, L., Têtu, B., Bergeron, A., McGraw, M., Staugaitis, S.M., Chabot, J., Hibshoosh, H., Sepulveda, A., Su, T., Wang, T., Potapova, O., Voronina, O., Desjardins, L., Mariani, O., Roman-Roman, S., Sastre, X., Stern, M.H., Cheng, F., Signoretti, S., Berchuck, A., Bigner, D., Lipp, E., Marks, J., McCall, S., McLendon, R., Secord, A., Sharp, A., Behera, M., Brat, D.J., Chen, A., Delman, K., Force, S., Khuri, F., Magliocca, K., Maithel, S., Olson, J.J., Owonikoko, T., Pickens, A., Ramalingam, S., Shin, D.M., Sica, G., Van Meir, E.G., Zhang, H., Eijckenboom, W., Gillis, A., Korpershoek, E., Looijenga, L., Oosterhuis, W., Stoop, H., van Kessel, K.E., Zwarthoff, E.C., Calatozzolo, C., Cuppini, L., Cuzzubbo, S., DiMeco, F., Finocchiaro, G., Mattei, L., Perin, A., Pollo, B., Chen, C., Houck, J., Lohavanichbutr, P., Hartmann, A., Stoehr, C., Stoehr, R., Taubert, H., Wach, S., Wullich, B., Kycler, W., Murawa, D., Wiznerowicz, M., Chung, K., Edenfield, W.J., Martin, J., Baudin, E., Bubley, G., Bueno, R., De Rienzo, A., Richards, W.G., Kalkanis, S., Mikkelsen, T., Noushmehr, H., Scarpace, L., Girard, N., Aymerich, M., Campo, E., Giné, E., Guillermo, A.L., Van Bang, N., Hanh, P.T., Phu, B.D., Tang, Y., Colman, H., Evason, K., Dottino, P.R., Martignetti, J. A., Gabra, H., Juhl, H., Akeredolu, T., Stepa, S., Hoon, D., Ahn, K., Kang, K.J., Beuschlein, F., Breggia, A., Birrer, M., Bell, D., Borad, M., Bryce, A.H., Castle, E., Chandan, V., Cheville, J., Copland, J.A., Farnell, M., Flotte, T., Giama, N., Ho, T., Kendrick, M., Kocher, J.P., Kopp, K., Moser, C., Nagorney, D., O'Brien, D., O'Neill, B. P., Patel, T., Petersen, G., Que, F., Rivera, M., Roberts, L., Smallridge, R., Smyrk, T., Stanton, M., Thompson, R.H., Torbenson, M., Yang, J.D., Zhang, L., Brimo, F., Ajani, J.A., Gonzalez, A.M.A., Behrens, C., Bondaruk, J., Broaddus, R., Czerniak, B., Esmaeli, B., Fujimoto, J., Gershenwald, J., Guo, C., Lazar, A.J., Logothetis, C., Meric-Bernstam, F., Moran, C., Ramondetta, L., Rice, D., Sood, A., Tamboli, P., Thompson, T., Troncoso, P., Tsao, A., Wistuba, I., Carter, C., Haydu, L., Hersey, P., Jakrot, V., Kakavand, H., Kefford, R., Lee, K., Long, G., Mann, G., Quinn, M., Saw, R., Scolyer, R., Shannon, K., Spillane, A., Stretch, O., Synott, M., Thompson, J., Wilmott, J., Al-Ahmadie, H., Chan, T.A., Ghossein, R., Gopalan, A., Levine, D.A., Reuter, V., Singer, S., Singh, B., Tien, N.V., Broudy, T., Mirsaidi, C., Nair, P., Drwiega, P., Miller, J., Smith, J., Zaren, H., Park, J.W., Hung, N.P., Kebebew, E., Linehan, W.M., Metwalli, A.R., Pacak, K., Pinto, P.A., Schiffman, M., Schmidt, L.S., Vocke, C.D., Wentzensen, N., Worrell, R., Yang, H., Moncrieff, M., Goparaju, C., Melamed, J., Pass, H., Botnariuc, N., Caraman, I., Cernat, M., Chemencedji, I., Clipca, A., Doruc, S., Gorincioi, G., Mura, S., Pirtac, M., Stancul, I., Tcaciuc, D., Albert, M., Alexopoulou, I., Arnaout, A., Bartlett, J., Engel, J., Gilbert, S., Parfitt, J., Sekhon, H., Thomas, G., Rassl, D.M., Rintoul, R.C., Bifulco, C., Tamakawa, R., Urba, W., Hayward, N., Timmers, H., Antenucci, A., Facciolo, F., Grazi, G., Marino, M., Merola, R., de Krijger, R., Gimenez-Roqueplo, A.P., Piché, A., Chevalier, S., McKercher, G., Birsoy, K., Barnett, G., Brewer, C., Farver, C., Naska, T., Pennell, N.A., Raymond, D., Schilero, C., Smolenski, K., Williams, F., Morrison, C., Borgia, J.A., Liptay, M.J., Pool, M., Seder, C.W., Junker, K., Omberg, L., Dinkin, M., Manikhas, G., Alvaro, D., Bragazzi, M.C., Cardinale, V., Carpino, G., Gaudio, E., Chesla, D., Cottingham, S., Dubina, M., Moiseenko, F., Dhanasekaran, R., Becker, K. F., Janssen, K.P., Slotta-Huspenina, J., Abdel-Rahman, M.H., Aziz, D., Bell, S., Cebulla, C.M., Davis, A., Duell, R., Elder, J.B., Hilty, J., Kumar, B., Lang, J., Lehman, N.L., Mandt, R., Nguyen, P., Pilarski, R., Rai, K., Schoenfield, L., Senecal, K., Wakely, P., Hansen, P., Lechan, R., Powers, J., Tischler, A., Grizzle, W.E., Sexton, K. C., Kastl, A., Henderson, J., Porten, S., Waldmann, J., Fassnacht, M., Asa, S.L., Schadendorf, D., Couce, M., Graefen, M., Huland, H., Sauter, G., Schlomm, T., Simon, R., Tennstedt, P., Olabode, O., Nelson, M., Bathe, O., Carroll, P.R., Chan, J. M., Disaia, P., Glenn, P., Kelley, R.K., Landen, C.N., Phillips, J., Prados, M., Simko, J., Smith-McCune, K., VandenBerg, S., Roggin, K., Fehrenbach, A., Kendler, A., Sifri, S., Steele, R., Jimeno, A., Carey, F., Forgie, I., Mannelli, M., Carney, M., Hernandez, B., Campos, B., Herold-Mende, C., Jungk, C., Unterberg, A., von Deimling, A., Bossler, A., Galbraith, J., Jacobus, L., Knudson, M., Knutson, T., Ma, D., Milhem, M., Sigmund, R., Godwin, A.K., Madan, R., Rosenthal, H.G., Adebamowo, C., Adebamowo, S.N., Boussioutas, A., Beer, D., Giordano, T., Mes-Masson, A.M., Saad, F., Bocklage, T., Landrum, L., Mannel, R., Moore, K., Moxley, K., Postier, R., Walker, J., Zuna, R., Feldman, M., Valdivieso, F., Dhir, R., Luketich, J., Pinero, E.M. M., Quintero-Aguilo, M., Carlotti, C.G., Dos Santos, J.S., Kemp, R., Sankarankuty, A., Tirapelli, D., Catto, J., Agnew, K., Swisher, E., Creaney, J., Robinson, B., Shelley, C. S., Godwin, E.M., Kendall, S., Shipman, C., Bradford, C., Carey, T., Haddad, A., Moyer, J., Peterson, L., Prince, M., Rozek, L., Wolf, G., Bowman, R., Fong, K.M., Yang, I., Korst, R., Rathmell, W.K., Fantacone-Campbell, J.L., Hooke, J.A., Kovatich, A.J., Shriver, C.D., DiPersio, J., Drake, B., Govindan, R., Heath, S., Ley, T., Van Tine, B., Westervelt, P., Rubin, M.A., Lee, J Il, Aredes, N.D., Mariamidze, A., Serody, J.S., Demicco, E.G., Disis, M.L., Vincent, B.G., Shmulevich, Ilya, 2018. The immune landscape of cancer. Immunity 48 (4), 812–830.e14.

Tourigny, D.S., Zucker, M., Kim, M., Russo, P., Coleman, J., Lee, C.H., Carlo, M.I., Chen, Y.B., Hakimi, A.A., Kotecha, R.R., Reznik, E., 2022. Molecular characterization of the tumor microenvironment in renal medullary carcinoma. Front. Oncol. 12, 1.

Trinh, M.K., Pacyna, C.N., Kildisiute, G., Thevanesan, C., Piapi, A., Ambridge, K., Anderson, N.D., Khabirova, E., Prigmore, E., Straathof, K., Behjati, S., Young, M.D., 2022. Precise identification of cancer cells from allelic imbalances in single cell transcriptomes. Commun. Biol. 5 (1).

Tsai, F.C., Kuo, G.H., Chang, S.W., Tsai, P.J., 2015. Ca2+ signaling in cytoskeletal reorganization, cell migration, and cancer metastasis. BioMed Res. Int. 2015.

V, I., Ai, K., PJ, M., R, V., 1993. Insulin-like growth factors (IGFs) and their receptors in adrenal tumors: high IGF-II expression in functional adrenocortical carcinomas. J. Clin. Endocrinol. Metab. 77 (3), 852–858.

Van Es, J.H., Sato, T., Van De Wetering, M., Lyubimova, A., Yee Nee, A.N., Gregorieff, A., Sasaki, N., Zeinstra, L., Van Den Born, M., Korving, J., Martens, A.C.M., Barker, N., Van Oudenaarden, A., Clevers, H., 2012. Dll1+ secretory progenitor cells revert to stem cells upon crypt damage. Nat. Cell Biol. 14 (10), 1099–1104, 1410. 2012 Sep. 23.

Vidal, V., Sacco, S., Rocha, A.S., Da Silva, F., Panzolini, C., Dumontet, T., Doan, T.M.P., Shan, J., Rak-Raszewska, A., Bird, T., Vainio, S., Martinez, A., Schedl, A., 2016. The

adrenal capsule is a signaling center controlling cell renewal and zonation through Rspo3. Genes Dev. 30 (12), 1389–1394.
Weiss, L.M., Medeiros, L.J., Vickery, A.L., 1989. Pathologic features of prognostic significance in adrenocortical carcinoma. Am. J. Surg. Pathol. 13 (3), 202–206.
Wilson, M., Koopman, P., 2002. Matching SOX: partner proteins and co-factors of the SOX family of transcriptional regulators. Curr. Opin. Genet. Dev. 12 (4), 441–446.
Xie, L., Wang, Q., Nan, F., Ge, L., Dang, Y., Sun, X., Li, N., Dong, H., Han, Y., Zhang, G., Zhu, W., Guo, X., 2019. OSacc: gene expression-based survival analysis web tool for adrenocortical carcinoma. Cancer Manag. Res. 11, 9145.
Yates, R., Katugampola, H., Cavlan, D., Cogger, K., Meimaridou, E., Hughes, C., Metherell, L., Guasti, L., King, P., 2013. Adrenocortical development, maintenance, and disease. Curr. Top. Dev. Biol. 106, 239–312.
Zheng, S., Cherniack, A.D., Dewal, N., Moffitt, R.A., Danilova, L., Murray, B.A., Lerario, A.M., Else, T., Knijnenburg, T.A., Ciriello, G., Kim, S., Assie, G., Morozova, O., Akbani, R., Shih, J., Hoadley, K.A., Choueiri, T.K., Waldmann, J., Mete, O., Robertson, A.G., Wu, H.T., Raphael, B.J., Shao, L., Meyerson, M., Demeure, M.J., Beuschlein, F., Gill, A.J., Sidhu, S.B., Almeida, M.Q., Fragoso, M.C.B. V., Cope, L.M., Kebebew, E., Habra, M.A., Whitsett, T.G., Bussey, K.J., Rainey, W.E., Asa, S.L., Bertherat, J., Fassnacht, M., Wheeler, D.A., Hammer, G.D., Giordano, T.J., Verhaak, R.G.W., Benz, C., Ally, A., Balasundaram, M., Bowlby, R., Brooks, D., Butterfield, Y.S.N., Carlsen, R., Dhalla, N., Guin, R., Holt, R.A., Jones, S.J.M., Kasaian, K., Lee, D., Li, H.I., Lim, L., Ma, Y., Marra, M.A., Mayo, M., Moore, R.A., Mungall, A.J., Mungall, K., Sadeghi, S., Schein, J.E., Sipahimalani, P., Tam, A., Thiessen, N., Park, P.J., Kroiss, M., Gao, J., Sander, C., Schultz, N., Jones, C.D., Kucherlapati, R., Mieczkowski, P.A., Parker, J.S., Perou, C.M., Tan, D., Veluvolu, U., Wilkerson, M.D., Hayes, D.N., Ladanyi, M., Quinkler, M., Auman, J.T., Latronico, A. C., Mendonca, B.B., Sibony, M., Sanborn, Z., Bellair, M., Buhay, C., Covington, K., Dahdouli, M., Dinh, H., Doddapaneni, H., Downs, B., Drummond, J., Gibbs, R., Hale, W., Han, Y., Hawes, A., Hu, J., Kakkar, N., Kalra, D., Khan, Z., Kovar, C., Lee, S., Lewis, L., Morgan, M., Morton, D., Muzny, D., Santibanez, J., Xi, L., Dousset, B., Groussin, L., Libé, R., Chin, L., Reynolds, S., Shmulevich, I., Chudamani, S., Liu, J., Lolla, L., Wu, Y., Yeh, J.J., Balu, S., Bodenheimer, T., Hoyle, A.P., Jefferys, S.R., Meng, S., Mose, L.E., Shi, Y., Simons, J.V., Soloway, M.G., Wu, J., Zhang, W., Shaw, K.R.M., Demchok, J.A., Felau, I., Sheth, M., Tarnuzzer, R., Wang, Z., Yang, L., Zenklusen, J.C., Zhang, J., Davidsen, T., Crawford, C., Hutter, C. M., Sofia, H.J., Roach, J., Bshara, W., Gaudioso, C., Morrison, C., Soon, P., Alonso, S., Baboud, J., Pihl, T., Raman, R., Sun, Q., Wan, Y., Naresh, R., Arachchi, H., Beroukhim, R., Carter, S.L., Cho, J., Frazer, S., Gabriel, S.B., Getz, G., Heiman, D.I., Kim, J., Lawrence, M.S., Lin, P., Noble, M.S., Saksena, G., Schumacher, S.E., Sougnez, C., Voet, D., Zhang, H., Bowen, J., Coppens, S., Gastier-Foster, J.M., Gerken, M., Helsel, C., Leraas, K.M., Lichtenberg, T.M., Ramirez, N.C., Wise, L., Zmuda, E., Baylin, S., Herman, J.G., LoBello, J., Watanabe, A., Haussler, D., Radenbaugh, A., Rao, A., Zhu, J., Bartsch, D.K., Sbiera, S., Allolio, B., Deutschbein, T., Ronchi, C., Raymond, V.M., Vinco, M., Amble, L., Bootwalla, M.S., Lai, P.H., Van Den Berg, D.J., Weisenberger, D.J., Robinson, B., Ju, Z., Kim, H., Ling, S., Liu, W., Lu, Y., Mills, G.B., Sircar, K., Wang, Q., Yoshihara, K., Laird, P.W., Fan, Y., Wang, W., Shinbrot, E., Reincke, M., Weinstein, J.N., Meier, S., Defreitas, T., 2016. Comprehensive pan-genomic characterization of adrenocortical carcinoma. Cancer Cell 29 (5), 723.
Zhou, Y., Zhang, X., Klibanski, A., 2012. MEG3 noncoding RNA: a tumor suppressor. J. Mol. Endocrinol. 48 (3).